Lithological Architecture and Petrography of the Mako Birimian Greenstone Belt, Kédougou-Kéniéba Inlier, Eastern Senegal

Moussa Dabo, Tahar Aïfa, Ibrahima Gning, Malick Faye, Mamadou Fallou Ba, Papa Malick Ngom

Accepted Manuscript

Lithological Architecture and Petrography of the Mako Birimian Greenstone Belt, Kédougou-Kéniéba Inlier, Eastern Senegal

Moussa Dabo, Tahar Aïfa, Ibrahima Gning, Malick Faye, Mamadou Fallou Ba, Papa Malick Ngom

PII:	S1464-343X(17)30148-6
DOI:	10.1016/j.jafrearsci.2017.04.005
Reference:	AES 2867
To appear in:	*Journal of African Earth Sciences*
Received Date:	19 September 2016
Revised Date:	01 February 2017
Accepted Date:	06 April 2017

Please cite this article as: Moussa Dabo, Tahar Aïfa, Ibrahima Gning, Malick Faye, Mamadou Fallou Ba, Papa Malick Ngom, Lithological Architecture and Petrography of the Mako Birimian Greenstone Belt, Kédougou-Kéniéba Inlier, Eastern Senegal, *Journal of African Earth Sciences* (2017), doi: 10.1016/j.jafrearsci.2017.04.005

- A detailed succession of the magmatic events within the Birimian Kédougou-Kéniéba Inlier is performed;
- Ultramafic rocks are included in the metabasalts in pillow lavas, therefore older;
- Amphibole-gneisses are now located at the upper part of the ultramafic rocks;
- Occurrence of a second generation of metagabbros (spotted) post-ribboned quarzites
- A general two-phase metamorphism reaching the amphibolite facies is evidenced;
- Andesitic to felsic mixed volcanism (explosive and effusive) on top of the new lithology;
- Succession of facies and geochemical results from literature assume an ophiolite of active margins.

Final version

Lithological Architecture and Petrography of the Mako Birimian Greenstone Belt, Kédougou-Kéniéba Inlier, Eastern Senegal

Moussa Dabo[1,2], Tahar Aïfa[2,*], Ibrahima Gning[1], Malick Faye[1], Mamadou Fallou Ba[1], Papa Malick Ngom[1]

[1] Département de Géologie, Faculté des Sciences et Techniques, Université Cheikh Anta Diop de Dakar, BP 5005, Dakar-Fann, Senegal

[2] Géosciences Rennes, CNRS UMR 6118, Université de Rennes 1, Bat.15, Campus de Beaulieu, 35042 Rennes Cedex, France

*Corresponding author: tahar.aifa@univ-rennes1.fr

Abstract

The new lithological and petrographic data obtained in the Mako sector are analyzed in the light of the geochemical data available in the literature. It consists of ultramaic, mafic rocks of tholeiitic affinities associated with intermediate and felsic rocks of calc-alkaline affinities and with intercalations of sedimentary rocks. The whole unit is intruded by Eburnean granitoids and affected by a greenschist to amphibolite facies metamorphism related to a high grade hydrothermalism. It consists of: (i) ultramafic rocks composed of a fractional crystallization succession of lherzolites, wehrlites and pyroxenites with mafic rock inclusions; (ii) layered, isotropic and pegmatitic metagabbros which gradually pass to metabasalts occur at the top; (iii) massive and in pillow metabasalts with locally tapered vesicles, completely or partially filled with quartzo-feldspathic minerals; (iv) quarzites locally overlying the mafic rocks and thus forming the top of the lower unit.

This ultramafic-mafic lower unit presents a tholeiitic affinity near to the OIB or N-MORB. It represents the Mako Ophiolitic Complex (MOC), a lithospheric fragment of Birimian lithospheric crust.

The upper unit is a mixed volcanic complex arranged in the tectonic corridors. From bottom to top it comprises the following: (i) andesitic, and (ii) rhyodacitic and rhyolitic lava flows and tuffs, respectively. They present a calc-alkaline affinity of the active margins.

Three generations of Eburnean granitoids are recognized: (i) early (2215-2160 Ma); (ii) syn-tectonics (2150-2100 Ma) and post-tectonics (2090-2040 Ma). The lithological succession,

geochemical and metamorphic characteristics of these units point to an ophiolitic supra-subduction zone.

Keywords: Birimian, Mako, lithology, ophiolites, pillow lavas, supra-subduction.

1. Introduction

The ~16000 km^2 triangular shape of Kédougou-Kéniéba Inlier (KKI) represents the westernmost exposed part of the Leo-Man Birimian terrane, which straddles the border between Senegal and Mali on the West African Craton (WAC) (Fig. 1). The Birimian terrane represents a major Paleoproterozoic juvenile crust-forming event during a time interval of 2.25-2.0 Ga (Taylor et al., 1988, 1992; Abouchami et al., 1990; Liégeois et al., 1991; Hirdes et al., 1992, 1996). The Birimian greenstone belts are mainly constituted of bimodal volcanic rocks with tholeiitic ultramafic-mafic complex overlapped by calc-alkaline intermediate-felsic complex, both intruded by tonalite-trondhjemite-granodiorite (TTG) plutons (Dia et al., 1997; Pouclet et al. 2006, Attoh et al., 2006; Dampare et al., 2008; Delor et al., 2010; Ngom et al., 2011).

The importance of the Birimian geology in the crustal evolution and the geodynamic significance of the WAC has been a subject of much debate. Some researchers suggested that Birimian juvenile crust production occurred largely in arc environments (Sylvester and Attoh, 1992; Ama Salah et al., 1996; Dia et al., 1997; Diallo, 2001; Pawlig et al., 2006), while others proposed that it was a plume generated (Abouchami et al., 1990; Hirdes and Davis 2002; Ngom et al., 2011). In the plume model, rapid crustal growth was accomplished by a mantle plume event which formed extensive oceanic plateaus, while the island arc setting accounts for basalts with MORB affinities assembled together with oceanic island arcs during subduction processes (Attoh et al., 2006).

Ophiolite rock assemblages characterized the relict fragments of oceanic crust and upper mantle, were mainly viewed as formed at mid-ocean ridges. They are recognized in some Birimian greenstone belts of the WAC (Pouclet et al., 2006, Attoh et al., 2006; Dampare et al., 2008). Ophiolite assemblages within belts of accreted terranes indicate an oceanic origin for some terranes, associated with volcanic arc and volcaniclastic material, granitoids, and silicic extrusives that make a mid-ocean ridge origin suspect (Hawkins, 2003). All geologic units that characterize ophiolites are found in supra-subduction zone (SSZ) rock assemblages, as well as containing distinctive rock types, such as boninite and island arc rock series (Hawkins, 2003; Pearce, 2003). SSZ ophiolites have the structures or inferred structures of oceanic crust,

yet a geochemical composition which indicates that they did not form mid-ocean ridges but at spreading centres associated with subduction zones (Pearce, 2003). Above the subduction zone, new oceanic crust is formed in the forearc, volcanic arc, and backarc basins (Hawkins, 2003). Paleoproterozoic Birimian greenstone belts of KKI are comprised of tholeiitic ultramafic-mafic basal complexes interstratified with calc-alkaline mafic-intermediate complex (Dia et al., 1997; Théveniaut et al., 2010; Ngom et al., 2011).

In this paper, we present new field and petrographic data of the Mako Birimian greenstone belt rocks in the westof KKI. The data were analyzed taking into account geochemical and geochronological data available in the literature (Diallo, 1994 Ngom, 1995; Dia et al., 1997; Gueye et al., 2008; Théveniaut et al., 2010). We propose a new lithological succession comprised of ultramafic-mafic tholeiitic basal complex with minor ultramafic rocks and major gabbro to basaltic rocks, surmounted by calc-alkaline intermediate-felsic complex made up of andesitic-dacitic-rhyodacitic and rhyolitic flows and pyroclastic rocks. Quartzitic lenses occurred interstratified with mafic rocks.

2. Geological framework of the WAC

The WAC (Fig. 1a) is dominated by volcanic and sedimentary Paleoproterozoic "Birimian" rocks (Taylor et al., 1988, 1992; Abouchami et al., 1990; Liegeois et al., 1991; Hirdes et al., 1992, 1996). In the Leo-Man shield, representing the southern part of the WAC, Birimian terranes consist of parallel and evenly spaced, NE-SW- to ENE-WSW- trending volcanic belts separated by sedimentary basins (Fig. 1a) and are coeval to slightly younger to emplacement of large granitoid plutons (Leube et al., 1990; Cheilletz et al., 1994; Pons et al., 1995). These Birimian terranes extend over more than two thirds of the eastern Man shield (Guinea, southern Mali, Ivory Coast, Ghana, Burkina Faso, southwestern Niger and northern Togo), the Kayes (in Mali) and KKI (Milési et al., 1989; Feybesse et al., 2006).

The lithological succession of the Birimian formations is very controversial. Some researchers (Junner, 1935; Milési et al., 1989, 1992; Ledru et al., 1991) proposed a predominantly sedimentary lower Birimian (B_1), and a volcanic and pyroclastic dominantly upper Birimian (B_2). Lateral equivalents of volcanic and sedimentary rock sequences were also envisaged (e.g. Leube et al. 1990; Hirdes et al. 1992). Recent radiometric dating of the volcanic and sedimentary units (Davis et al., 1994; Doumbia et al., 1998; Lüdtke et al., 1998, 1999; Dia et al., 1998; Hirdes and Davis, 2002; Théveniaut et al., 2010) places the major period of accretion of juvenile mafic volcanic-plutonic rocks around 2.25-2.17 Ga, whereas the

Birimian sedimentary activity occurred at 2.15-2.10 Ga (Abouchami et al., 1990; Bassot, 1997; Feybesse et al., 2006).

The Birimian formations were deformed during the 2.1-2.0 Ga Eburnean orogeny (Bonhomme, 1962; Abouchami et al., 1990; Liégeois et al., 1991; Boher et al., 1992; Taylor et al., 1992). Eburnean tectono-magmatic events are interpreted by some authors as a single progressive deformation event involving compression along a NW-SE axis (Eisenlohr and Hirdes, 1992; Blenkinsop et al., 1994). For others, the evolution is polycyclic including three major phases of deformation: D_1, collisional (Ledru et al., 1989, 1991; Milési et al., 1992), peri-plutonic deformations (Vidal et al., 1996; Pouclet et al., 1996) or vertical tectonics of unconstrained side diapirs (Vidal et al., 2009; Lompo, 2010), and D_2 and D_3 transcurrent faulting (Milési et al., 1989; Feybesse et al., 1989; Dabo and Aïfa, 2011). The metamorphism related to the Eburnean orogeny in the Birimian formations of the WAC is of mesozonal facies (Klemd et al., 2002; Block et al., 2015) before being locally overprinted by epizonal facies (Dia, 1998; Debat et al., 2003; Block et al., 2015). Eburnean deformation features host the majority of the gold deposits, which generally occur aligned along major tectonic zones (Milési et al., 1989, 1992; Liégeois et al., 1991; Feybesse et al., 2006; Dabo et al., 2015).

3. Geology of Kédougou-Kéniéba Inlier

The Paleoproterozoic Birimian of the KKI consists of volcanic, volcano-sedimentary, and sedimentary formations, which are distributed into two supergroups (Bassot, 1987): the Mako Supergroup to the west and the Dialé-Daléma Supergroup in the east, separated by a crustal-scale shear zone, the Main Transcurrent Zone (MTZ) (Fig. 1b).

The Mako Supergroup is composed of bimodal volcanoplutonic sequences (Ngom, 1995; Dia et al., 1997) with ultramafic bodies associated with submarine volcanism at the bottom and andesitic flows with abundant pyroclastites and volcano-detrital rocks at the upper parts of the pile.

The bimodal volcanic belts consist successively of tholeiitic and calc-alkaline rocks (Dia, 1988; Ngom, 1995). The tholeiitic sequences at the bottom of these belts are mainly represented by pillow basalts and/or none structured basaltic flows with N- or T-MORB affinities and large slices of ultramafic-mafic rocks (Dia et al., 1997; Delor et al., 2010). The mafic rocks (metabasalts and metagabbros) and the ultramafic rocks exhibit comagmatic geochemical and lithological features (Ngom, 1995). The calc-alkaline volcanism is composed of andesitic to felsic rocks with abundant pyroclastics interstratified with volcano-detrital material (Diallo, 1994; Ngom, 1995; Dia et al., 1997).

The volcanic assemblage is dated between 2170 and 2213 ± 3 Ma (Abouchami et al., 1990, Dia et al., 1997; Gueye et al., 2007). The volcanic packages and the granitoids are interpreted to have island arc affinities on the basis of geochemical and petrological constraints (Dia, 1988; Diallo et al., 1993; Diallo, 1994; Dia et al., 1997; Pawlig et al., 2006) or represent mantle plume assemblageultramafic-mafic rocks followed by orogenic volcanic arc assemblages for the calc-alkaline complex (Bassot, 1987; Abouchami et al., 1990; Hirdes et Davis, 2002; Ngom et al., 2010).

The Dialé-Daléma Supergroup, in contrast with the Mako Supergroup, is composed primarily of turbiditic and carbonated metasediments, and is cross-cut by volcanic complex, which is mainly made up of andesitic and rhyolitic rocks (Milési et al., 1986, 1989; Dommanget et al., 1993; Dabo and Aïfa, 2010).

Detrital sedimentary rocks of Dialé-Daléma in the Loulo district have been dated between 2098 ± 11 Ma and 2125 ± 17 Ma (Boher et al., 1992) and detrital zircons from a quartz wacke gave an average age of 2165 ± 1 Ma for the source rocks (Hirdes and Davis, 2002). A rhyolite flow Unit from the southern parts of the Dialé-Daléma Supergroup has been dated at 2099 ± 4 Ma (Hirdes and Davis, 2002).

The Birimian volcanic, volcano-sedimentary and sedimentary rocks of the Mako and Dialé-Daléma Supergroups are intruded by several generations of Eburnean granitoids, which form three batholiths: Badon-Kakadian, Saraya and Boboti (Bassot, 1966; Dia et al., 1997). The Badon-Kakadian batholith consists of a complex suite of pre- and syn-tectonic mafic to felsic rocks, dated in the range of 2080-2213 Ma (Dia, 1988; Dia et al., 1997; Gueye et al., 2007). The Saraya and Boboti batholiths consist of calc-alkaline syn-tectonic I-type, hornblende-biotite-bearing TTG granitoids with ages ranging between 2100-2060 Ma (Saraya) and 2080-2060 Ma (Boboti) (Hirdes and Davis, 2002; Gueye et al., 2007; Delor et al., 2010). Théveniaut et al. (2010) assembled these batholiths into three suites: Sandikounda-Soukouta (2170-2140 Ma), Saraya (2100-2060 Ma) and Boboti (2080-2060 Ma).

The metamorphism of Birimian formations of the KKI is mostly in the greenschist facies, but amphibolite facies can be found locally, such as in the Sonfara-Sandikounda amphibolitic-gneissic complex and around some plutons (Bassot, 1966; Dia et al., 1997).

Structural studies distinguish generally three major phases of Eburnean deformation (D_1, D_2 and D_3) in the KKI (Ledru et al., 1989, 1991; Dabo and Aïfa, 2011): D_1 of compressional tectonics (thrusting), D_2 transcurrent or transpression tectonics with NS to NE-SW sinistral strike-slip faults and D_3 dextral transcurrent or transtension tectonics. D_2 is associated with

two large NS- to NE-trending tectonic contacts: the Senegalo-Malian Fault (SMF) in the Dialé-Daléma Supergroup (Bassot and Dommanget, 1986; Bassot 1987; Dabo, 2011) and the MTZ, which marks the limit between both the Mako and Dialé-Daléma Supergroups (Fig. 1b).

This paper is a contribution to the lithostratigraphic and geodynamic debate on the KKI Birimian terranes. The results presented below bring new field and petrographic data which requires a reconsideration of the existing lithologic and geodynamic models suggested for the Mako Supergroup.

4. Lithological architecture of Mako

The Mako Sector, in the northern part of Mako Supergroup (Fig. 1b), is a metamorphic assemblage zone primarily made up of ultramafic, mafic, intermediate and felsic rocks associated with quartzites (Fig. 2a). Mafic rocks are the most significant and constitute the main part of the greenstone hills between Seguéko Fulani to the north and Wassadou to the south. Beside the hills made up of greenstone belt mafic rocks also exposed are black ultramafic rocks of Koulountou and of Manssari-Tana forming topographic highs, to the east and west of Mako village, respectively. Kilometric lenses of quarzites, oriented NW-SE and NE-SW, are inserted locally between the mafic rocks. Andesitic breccias and felsic lavas occupy the tectonic corridors cross-cutting the ultramafic, mafic and quartzites rocks. All these formations are cross-cut by several generations of plutons (granitoids and gabbros) which constitute the main part of the outcrops in Niéméniké village (Fig. 2). On the EW cross-section, between Lamé and Badian villages (Fig. 2b), ultramafic rocks, layered gabbros, pegmatitic gabbros and isotropic gabbros follow one another gradually with a sharp regular subvertical contacts. In the tectonic corridor of Bafoundou, the gabbros are cross-cut by red andesitic breccias which pass laterally to quarzites then to pillow basalts in the neighbourhoods of the Badian village. The contact between ultramafic rocks, gabbros and basalts is progressive. On the other hand, fault contacts separate the ultramafic-mafic rocks from the andesitic breccias and quarzites. On the NW-SE cross-section (Fig. 2c), between Lamé and Sékhoto Peul, a lithologic succession, almost similar to that of the previous section is exposed. However, the andesitic breccias give way to rhyolitic breccias and rhyolitic lavas of the Mako Supergroup which cross-cut the metabasalts. These metabasalts, often appear as pillow lavas, are common towards Sékhoto Peul. In addition, several generations of plutonic intrusions (granitoids and gabbros) with variable tectonic fabrics, were emplaced into the volcanic and volcano-sedimentary units between Niéméniké and Sékhoto Peul (Fig. 2).

The space distribution and the geometrical relations between the various lithological facies, enable us to distinguish two lithological units: the ophiolitic complex at the base and the mixed volcanic complex at the top, separated by the lenses of quarzites.

4. 1. The Mako Ophiolitic Complex

The Mako Ophiolitic Complex (MOC) consists of partially serpentinized ultramafic rocks associated with metagabbros, amphibole-gneiss, massive and pillow metabasalts and the overlying quarzites.

Ultramafic rocks

Ultramafic rocks outcrop in the hills of Koulountou and of Manssari-Tana (Fig. 3a), in the shape of polygonal blocks and boulders of variable sizes. The rock surface is red to ochre in colour and exhibits severe alteration (Fig. 3b). On a fresh surface, it has a fine grained texture; balck with phenocrysts of pyroxenes associated with some greenish olivine grains. The olivines are alterated to a whitish crust of serpentine (Fig. 3b).

Under the microscope, the rocks comprise metaperoditites (wehrlites and lherzolites) and metapyroxenites (websterites). The lherzolites show an abundance of olivines and pyroxenes set in a heteradcumulate texture (Fig. 3c). Magnesian olivines and orthopyroxenes are often altered into serpentine and opaque minerals. Clinopyroxenes are partly transformed into amphibole (actinote), chlorite and calcite. Some chromite crystals appear locally. The wehrlites are characterized by clinopyroxenes which occupy the interstices between the cracked olivine crystals. In the cracks also occur recrystallized serpentine and opaque minerals.

Pyroxenites are mainly websterites, which are mostly composed of both orho- and clino-clinopyroxenes and opaque minerals. The clinopyroxenes are generally transformed into amphibole, chlorite and calcite. These metapyroxenites as well as some metagabbros result from the differentiation by fractionated crystallization of the ultramafic magma (Ngom, 1995).

Metagabbros and amphibole-gneisses

Metagabbros often crop out at the base of the hills of metabasalts and are associated with ultramafic rocks towards the top and laterally (Fig. 3a). They are almost confined between the hills of ultramafic rocks with metagabbros to the east and the metabasalts to the west of Mako. They have several equant (isotropic), pegmatitic with comb-layered textures (Lofgren

238 and Donaldson, 1975; Figs. 3d,e). The isotropic metagabbros are more abundant and crop out
239 mainly in the centre and west of Mako. They are characterized by a coarse grained texture
240 with grains of amphibole, pyroxene, chlorite, plagioclase, quartz and opaque minerals (Fig.
241 3d). The coarse grained pegmatitic grabbros are more abundant towards the SE. They often
242 show a comb-layered texture (Lofgren and Donaldson, 1975) with phenocrysts of
243 clinopyroxene arranged in sheaves (Fig. 3e) leaving meshs occupied by plagioclases and
244 secondary minerals (quartz, epidote, calcite and opaque minerals). These pegmatitic gabbros
245 are a result of the differentiation of websterites and are marked by the increase in the modal
246 composition of oxides and the increase in the size of minerals in the rock (Ngom, 1995).
247
248 In the SE part (towards Lamé) hectometric massifs of layered metagabbros conformably
249 outcrop on the ultramafics and the pegmatitic gabbros (Fig. 3f). Under polarizing microscope
250 they appear like amphibole-gneisses with granolepidoblastic texture, characterized by an
251 alternation of light feldspathic minerals and ferromagnesian minerals (mainly pyroxenes,
252 amphiboles and chlorites) (Fig. 3g). Plagioclases represent the main part of light minerals and
253 are sometimes transformed into calcite, epidote and quartz. Quartz occurs in the form of
254 microcrystals dispersed in the interstices between other minerals. In the mafic units, the
255 amphiboles are more abundant and consist mainly of secondary hornblende and actinolite.
256 They are sometimes transformed into layers of chlorite adjacent to the amphibole needles.
257 Clinopyroxenes, partially transformed into amphibole and calcite, are disseminated in the
258 background of the thin section. Rare orthopyroxenes and olivines partially altered into
259 serpentine, appear in the ferromagnesian mineral. Some grains of epidote, sphene and needles
260 of damourite supplement the mineralogy of these amphibole-gneisses. These amphibole-
261 gneisses described for the first time in the Mako Sector, testify an amphibolite degree of
262 metamorphism. The metagabbros pass in general gradually to metabasalts at the top with
263 hardly discernible diffuse limits even sometimes of interpenetrations between both facies
264 (Fig. 3d).
265
266 ***Metabasalts***
267 The metabasalts occupy mainly the top of the hills of greenstone rocks bordering the Mako
268 village (Figs. 2,3a). On the front wall of the quarry of the Sahelian Enterprises Co., the
269 metagabbros pass gradually into massive metabasalts then in pillow basalts at the top (Figs.
270 4a,b). These pillow lavas locally contain black enclaves of metaperidotites (Fig. 4c) made up
271 of layered serpentines associated with some secondary calcite crystals and opaque minerals

(Fig. 4e). Massive metabasalts, often with amygdalae structures (Figs. 3d,4), outcrop mainly in the eastern part of Mako village where they are found on top of the metagabbros in some areas. The rock has a microlithic texture with a chloritized mesostase which appear as plagioclase microliths associated with rare secondary quartz grains and pyroxene relics (Fig. 4d,e). The amygdalae locally abundant comprises elliptical vesicles filled up with hydrothermal paragenesis with quartz, feldspar, chlorite, epidote (Fig. 4d).

The more frequent metabasalts in the hills of the western part of Mako show pillows (Figs. 4a,b) of variable size ranging from centimetric to metric. The pillow basalts generally sit on top of or are interstratified with the massive metabasalts (Figs. 4d,e). In the pillow metabasalts appear ribboned tension gashes which are partially filled up by the same paragenesis as that of the amygdalas in the massive metabasalts. In the shear zones, the metabasalts are transformed into chloritoschists exhibiting the following secondary mineralogy: chlorite, epidote, feldspar, quartz and opaque minerals (Fig. 4f). The pillow metabasalts are overlain locally by lenses of ribboned quarzites.

Quartzites

The quarzites form hills defined by lenticular beds that are stretched and "boudinaged" within the mafic rocks. The thickness of the beds is variable and exceeds 500 m in some places. At the outcrop, the primary bedding is defined by an alternation of light and dark centimetric beds (Fig. 5a). The texture is granoblastic, mainly made up of microgranular quartz associated with some sericite needles (Fig. 5b). The light beds are composed of quartz and dark beds of quartz and reddish iron oxides, similar to jasperoids. Locally, conglomeratic quartzites with rare centimetric rollers are also exposed. The rollers are dark and deformed and in thin section are made up of chlorite and sericite (damourite) associated with secondary greyish quartz.
The quarzites constitute the sedimentary cover of the metabasalts and metagabbros and represents recrystallized and deformed jaspers with radiolarians. In addition, some N160° oriented quarzites bands show minor ferromagnesian mineral relics (epidote, chlorite) suggesting an origin related to intense silicification of old magmatic rocks.

4.2. The Mixed Volcanic Complex

It consists of a mixed volcanism (explosive and effusive) represented by breccias and andesitic, rhyodacitic and rhyolitic lavas, which crop out in tectonic corridors between Mako and Bafoundou villages. These volcanites are injected into the rocks of the MOC (Fig. 2).

Andesitic breccias and lavas

The andesitic breccias consist of polygenic rock fragments of variable sizes (millimetric to centimetric) and rock type (sedimentary, magmatic) mainly of magmatic origin. These lithoclasts, with subround shapes occur in the shear zones whereas the angular lithoclasts occur outside the shear zone. The lithoclasts are packed in a fresh greenish or reddish brown mesostase (Figs. 6a,b). Grain sorting of the lithoclasts (Fig. 6b) is perceptible at certain places and shows local lithologic inversions due to deformation. They locally show cross-bedding, channelling features characteristics of fluviale deposition (Fig. 6a). In thin section, one can observe microlithic lithoclasts within a cement entirely recrystallized out of quartz, feldspar, chlorite and epidote (Fig. 6c,d). The fine mafic grained enclaves are metagabbroic with crystals of amphibole, clinopyroxene, chlorite and feldspar (Fig. 6b). In spoil of a well dug on the level of a shear zone west of Mako village, the rock is transformed at depth into chloritoschists of porphyritic lepidogranoblastic texture with an alternation of phyllitic beds (with chlorite and sericite) and quartzo-sericitic beds, containing lithoclasts of quarzite, basalt and peridotite (Fig. 4f).

The andesitic breccias are interstratified with andesitic lavas which locally constitute sharpened hills in particular to the NW of Mako village. The lavas are distinguished by the presense of plagioclase and amphibole phenocrysts in a greenish mesostase (Fig. 6d). The texture is microlithic porphyritic with plagioclase microliths associated with some opaque minerals in a mesostase strongly recrystallized out of chlorite and epidote. Feldspars form poecilitic phenocrysts of twinned plagioclases and some with Carlsbad twinned sanidines are common.

Breccias and rhyolitic and rhyodacitic lavas

The breccias and andesitic lavas west Mako pass gradually to rhyolitic and rhyodacitic breccias to the east Mako. These rocks are coarser in the west and become increasingly finer towards the east. The contact between the andesitic and rhyolitic breccias seems progressive even though no contact was observed between the two facies. The rhyolitic lavas are abundant close to the pink granite of Niéméniké (Fig. 2). They are interstratified with rhyolitic breccias which show magmatic bedding with an alternation of fine siliceous grains and horizons made up of medium feldspathic grains (Fig. 6e). In the shear zones, they are mylonitized and transformed into sericitoschists (Fig. 6f). Feldspar and quartz coarse grains are packed within

339 the foliation. Some red trails of oxide and the feldspathic koalinitization underline major
340 schistosity.
341 In the SE part, the breccias and rhyolitic lavas are associated with breccias and rhyodacitic
342 lavas. They show a porphyritic microlithic texture with feldspar phenocrysts (plagioclase and
343 sanidine) in a mesostase strewn with plagioclase microliths, biotite and chlorite layers, as well
344 as grains of epidote and quartz. The whole of these Birimian ultramafic, mafic, intermediate
345 and felsic formations is cross-cut by the Eburnean granitoid intrusions.
346
347 **4.3. Eburnean granitoids**
348 The granitoids of the Mako Sector consist of diorites, granodiorites and granites. They form
349 several generations of massifs with variable dimensions, which are intrusive into the
350 ophiolitic and mixed volcanic complexes (Fig. 2). According to their age, their relationships
351 to the Birimian formations and the Eburnean deformation, three groups of massifs can be
352 distinguished: (i) early granitoids π1 (2200 Ma to 2160 Ma), deformed and intrusive into the
353 greenstone belts; (ii) conformable syn-tectonic granitoids π2 (2150 Ma to 2100 Ma); (iii) and
354 subarounded post-tectonic granitoids π3 (2090 Ma to 2040 Ma). These last two groups are
355 intrusive into the greenstone belts and the sedimentary Birimian basins.
356
357 ***Early Granitoids π1*** are represented in the Mako Sector by the Soukourtou microgranite with
358 biotite cross-cut by granodiorite with mafic enclaves (Fig. 7a). At the outcrop, the pinkish
359 coloured rock presents a fine granulometry and an intense deformation underlined by a
360 folding and a rough foliation (Fig. 7a). The mineralogy is mainly composed of microcrystals
361 of quartz, feldspar and biotite organized in a microgranular and even granoblastic texture with
362 a rough foliation underlined by the alignment of some partially chloritized biotite layers.
363 Muscovite, epidote and opaque minerals supplement the mineralogy of the rock (Fig. 7b).
364 This microgranite underwent the effect of contact metamorphism related to the emplacement
365 of the granodiorite with mafic enclaves which involved its deformation and its transformation
366 into orthogneiss (Fig. 7a).
367 This granite with orthogneiss biotite would represent a part of the granodiorite of Badon
368 located ~3 km northward and dated by $^{207}Pb/^{206}Pb$ method on zircon at 2213 ± 3 Ma
369 (Gueye et al., 2007). This early plutonism emplaced subsequently to the ophiolitic complex
370 of the Mako Sector. This emplacement occurred during the first phase of Eburnean
371 deformation D_1 which involved in pillow basalts a ductile deformation (folding) while the
372 rock was not completely cool.

Syn-tectonic granitoids π2 are the massifs elongated according to NE-SW to NS Eburnean directions and often containing mafic enclaves. They show a planar anisotropy marked by the stretching of quartzo-feldspathic grains according to a foliation underlined by phyllitic minerals. In the study area, they are represented by the granodiorites of Soukourtou (Fig. 7a) and the curve of Sékhoto Peul along the RN7 road as well as mesocrat diorite of Niéméniké (Fig. 2).

The granodiorite of Soukourtou is leucocratic, but locally blended of mafic enclaves which confers it a mesocrat aspect. On its western edge, the granodiorite is injected or in contact with the orthogneissified microgranite. Its contact with the metabasalt is irregular, which assumes a contemporaneous to sub-contemporaneous emplacement. On thin sections, millimeter-length crystals of quartz, alkaline feldspars (orthoclase, microcline), plagioclase and lengthened layers of biotite and amphibole can be distinguished. The leucrocrat granodiorite of the curve of Sékhoto Peul along the RN7 road also presents mafic enclaves. It shows grains of quartz (~30%), plagioclase (~35%), alkaline feldspar (~5%) and layers of biotite (~12%) and amphibole (~10%) lengthened according to the foliation direction (Fig. 7a). The texture is mainly grained, but locally becomes microgranular, particularly in the vicinity of the enclaves. In the parts rich in enclaves, the rock becomes mesocrat because of the rate increase of ferromagnesian minerals coming from the mafic facies.

The mafic enclaves of the granodiorites are generally deformed (boudinaged, sheared, twisted) with irregular limits (Figs. 7d,e). They are mostly made up of secondary amphiboles (~65%) associated with quartz and feldspars (Fig. 7e). Rare relics of olivine and orthopyroxene developing a rim of green alteration with epidote, can be observed. In the granodiorite of Sékhoto Peul, the mafic enclaves are transformed into dark diorite. The limits between minerals of the enclaves and those of the granodiorite are diffuse (Fig. 7d). In some places, minerals of the enclaves are isolated within minerals from the granodiorite and vice versa (Fig. 7f). Moreover, injections of the granodiorite appear in the fractures of the enclaves (Fig. 7d).

In the granodiorite of Sourkoutou the mafic enclaves are metagabbros showing a microgranular rim reaction separating them from the granodiorites (Fig. 7e). These granodiorites with mafic enclaves would be related to an incomplete mixture (mingling) between a mafic magma and the felsic magma with faster cooling of the less viscous mafic magma (Pitcher, 1993; Nédélec and Bouchez, 2011).

In addition, a mesocrat diorite outcrops in Niéméniké at about 1 km SE of the Soukourtou granodiorite. The rock shows a grained texture made up of centimetric plagioclase and

amphibole rods, intermingled with some quartz and biotite. It is slightly deformed with a rough anisotropy, tension gashes and fractures. These fractures are secondarily borrowed by primarily feldspathic aplitic arrivals.

In chronological viewpoint, these diorites and granodiorites would be the equivalent of the granodiorite of Soukouta, located at about 5 km westward, dated by U/Pb on zircon at 2142 ± 7 Ma (Delor et al., 2010).

Post-tectonic granitoids π3 form the subarounded massifs with equant texture often without enclaves and unconformable on Eburnean structures. They are represented by the pink granite of Niéméniké, made up mainly of alkaline feldspars such as orthose, associated with bluish quartz and plagioclase. The ferromagnesian minerals are represented by needles of amphibole and mica layers (muscovite and biotite). The deformation is primarily brittle but some small shear corridors appear locally. Pegmatic and aplite dykes and intrusions of spotted grabbros are injected into the rock fractures (Fig. 8a). These post-tectonic granites can be chronologically related to that of Tinkoto located at around 7 km southward and dated by U/Pb method on zircon at 2074 ± 9 Ma (Gueye et al., 2007).

The late spotted gabbros are dykes and late gabbros massifs, mottled fine needles of pyroxenes ouralitized in amphiboles which draw a dark mineral lineation (Fig. 8a). They outcrop in Niéméniké, and are locally dioritic and cross-cut the quarzites and the late granitoids. The dykes of various sizes and orientations, are localized along the fractures of limited extension. They are locally deformed and are different from the Paleoproterozoic dykes reported on the WAC by Jessel et al. (2015). Under the microscope, from the amphibole layers, pyroxene relics (orthopyroxenes and clinopyroxenes) partially chloritized and epidotized associated with some quartz crystals, feldspars and of opaque minerals are distinguished (Fig. 8b). In the most deformed terms, the rock is connected with foliated dioritic metagabbros. Quartz and feldspar become more abundant and form clear beds with recrystallized fine grains alternating with the dark beds of amphiboles and pyroxenes (Fig. 8c). The texture evolves from grained to nematogranoblastic according to localization or not of the rock in the shear zones (Fig. 8b,c).

The age of these mottled gabbros is not yet defined. However, our observations suggest an age younger than that of post-tectonic granitoid they cross-cut (Fig. 8a). The foliation of the mottled gabbros could be related to a late Eburnean deformation phase (D_3) which occurred during the emplacement of these gabbros. The granitoids already exhibit a semi-ductile deformation and occur along a corridor with moderate shearing. The gabbroic dykes are injected into the semi-ductile structures.

Finally, note that the syn- and post-tectonic granitoids appear in the greenstone belt rocks as well as in the Birimian sedimentary basins, contrary to early granitoids which cross-cut only the greenstones. Moreover, the ductile deformation is more important in the syn-tectonic granitoids whereas post-tectonic granitoids are equant with a ductile deformation confined in microcorridor shears.

5. Discussion and conclusions

The Birimian formations of the Mako sector consist of ophiolitic and mixed volcanic complexes showing a bimodal geochemical character (tholeiitic and calc-alkaline), separated by a jasperoid horizon and cross-cut by a series of Eburnean granitoids. The unit is metamorphozed in the amphibolite greenschist facies.

The Mako Ophiolitic Complex

Ultramafic rocks in the Mako Sector are differentiated into wehrlite, lherzolite, websterite, pyroxenite and gabbro with a magmatic bedding related to a fractionated crystallization (Ngom, 1995). They present a tholeiitic affinity and are depleted in REE (Delor al., 2010). Their age is not yet known however they are included in the metabasalts dated by Sm/Nd (WR) between 2197 ± 13 Ma and 2195 ± 11 Ma (Dia, 1988). Other datings are needed to fix the age of these metabasalts of the Mako Supergroup. Moreover, the granodiorite of Badon dated by $^{207}Pb/^{206}Pb$ at 2213 ± 3 Ma (Gueye et al., 2007) intrudes the Mako Birimian greenstone belt, thus predicting an older age for the ultramafic rocks. In the Birimian of Ghana, the age of the ultramafic rocks is supported by the field relations, as well as the 2159 ± 4 Ma age of the granitoid intruded into the western flank of the ultramafic-greenstone belt complex (Attoh et al., 2006). These ultramafic rocks at the base of a Birimian ophiolitic fragment of the KKI are considered as the diagnosis of subduction tectonic settings (Peters et al., 1991; Pearce, 2003; Attoh et al., 2006; Dampare et al., 2008).

The ultramafic rocks are topped by metagabbros which form with the metabasalts the main part of the greenstones hills (Fig. 9). The metagabbros have variable textures and often occupy the base of such hills, on top of which metabasalts outcrop. Their geochemistry and age are similar to those of metabasalts with which they would be cogenetic (Ngom et al., 2011).

Amphibole-gneisses result from metamorphism of the metagabbro base. They present a paragenesis to quartz, feldspar, amphibole, chlorite, pyroxene and epidote (Table 2), characteristic of the amphibolite facies. This facies would be related to a prograde metamorphism former to retrograde greenschist metamorphism, following the example of the other Birimian provinces of the WAC (Klemd et al., 2002; Block et al., 2015). They are

interpreted as the result of an oceanic basaltic crust subduction (Pawlig et al., 2006) and illustrate a transition between Archean and Phanerozoic orogens (Klemd et al., 2002; Block et al., 2015).

In Ghana, the pressure-temperature conditions obtained in the Birimian amphibolite facies are of 500-680°C at 4.5-10 Kbars (Klemd et al., 2002; Block et al., 2015). This amphibolite facies metamorphism is followed by retrograde greenschist-facies conditions at temperatures of 400-540°C associated with hydrothermal alteration and gold mineralization (Klemd et al., 2002). The age of the Mako amphibolites is not defined, however, the old zircons obtained on the tonalitic gneiss from Sandikounda are dated at 2194 ± 4 Ma (Gueye et al., 2007). In Ghana, the U-Pb ages on monazite obtained on the amphibolite metamorphism are estimated between 2138 ± 7 Ma and 2130 ± 7 Ma (Block et al., 2015).

In addition, in the Mako Sector, the gradient of metamorphism locally varies from SE towards NW, passing from the amphibolite facies to greenschist facies. In the shear zones, the metamorphic conditions are more pronounced.

The metabasalts in pillow lavas are directly topped by massive metabasalts (Figs. 4a,9). These two types of metabasalts would be comagmatic (Ngom, 1995), and show a lithological continuity and a narrow space association in the field. Both let appear a tholeiitic geochemical affinity with however slightly an enrichment in elements, strongly hygromagmaphiles and LREE for massive basalts (Ngom, 1989; Ngom et al., 2011).

The origin of the enrichment of massive basalts in elements strongly hygromagmaphiles and LREE is discussed. It could be related to post-magmatic contaminations (hydrothermalism, metamorphism, deformation) in particular with the intense hydrothermalism associated with the penetrative amygdalae structures (Fig. 3d). For Pawlig et al. (2006), the plumes could be responsible for the partially enriched character of the tholeiitic basalts.

In former research works, the metabasalts in pillow lavas and the metagabbros (depleted tholeiites) are comparable with N-MORB or oceanic plateau basalts (Dia 1988; Abouchami et al., 1990; Ngom, 1995; Théveniaut et al., 2010; Ngom et al., 2011), whereas the massive metabasalts (enriched tholeiites) are comparable with the arc (Ngom, 1989). However, in the $TiO_2/Fe_2O_3/MgO$ diagrams of Miyashiro (1974); Ti/Cr of Pearce (1975) and Cr/Y of Pearce et al. (1980), geochemical data obtained on most ultramafic, mafic and intermediate rocks of the Mako Supergroup (Ngom, 1995) are located in the SSZ field (Fig. 10).

Hectometric lenses of jasperoid quarzites which represent old jaspers with radiolarians constitute the sedimentary covers of the ultramafic and mafic rocks (Fig. 5). However, quarzites containing ferromagnesian mineral relics could be associated with a silicification of

old magmatic rocks. This lithologic succession of ultramafic and mafic rocks with tholeiitic character covered by jasperoid sediments (Fig. 9) is related to a Birimian ophiolitic sequence in the Mako sector following the example of the Birimian ophiolitic sequences of the WAC (Attoh et al., 2006; Pouclet et al., 2006; Dampare et al., 2008). We named it Mako Ophiolitic Complex (MOC). However, the dyke swarm complex often associated with the ophiolites has not been observed neither in the field nor on the aeromagnetic map (Aïfa and Dabo, 2011).

The MOC is cross-cut by faults through which Mixed calc-alkali Volcanic Complex is emplaced. Indeed, the lavas and breccias of meta-andesites, meta-rhyodacites and meta-rhyolites are interstratified in tectonic corridors open within the MOC (Fig. 2). The breccias and lavas of meta-andesites represented westwards pass towards the east to breccias and to interstratified rhydacitic and rhyolitic lavas. These formations of mixed volcanism slightly show a calc-alkaline affinity weakly to strongly potassic of subduction zones (Dia, 1988; Abouchami et al., 1990; Ngom, 1995; Théveniaut et al., 2010; Ngom et al., 2011). The andesites of the Mako Supergroup gave an Sm/Nd (WR) age of 2160 ± 16 Ma (Boher, 1991).

The Birimian formations were intruded by granitoids classified into three groups: (i) early π1, in the greenstone belt rocks between 2215 Ma and 2160 Ma, and (ii) conformable syn-tectonic π2 and (iii) unconformable post-tectonic π3 emplacements in the basins and greestone belt rocks, during the periods 2150-2100 Ma and 2090-2040 Ma, respectively. These different granitoids are mainly in the field of calc-alkaline magmatism of subduction zones (Delor et al., 2010). Late mottled gabbros cross-cut the granitoids (Fig. 8a). These gabbros were emplaced during the last Eburnean deformation phase in zones of weak extension.

All that precedes, let predict that the southernmost part of the Mako Supergroup would consist of at least two distinct magmatic events (tholeiitic and calc-alkaline) following a polycyclic evolution in an SSZ context (Pearce, 2003) as for other Birimian provinces of the WAC (Béziat et al., 2000; Attoh et al., 2006; Dampare et al., 2008; Lompo, 2009).

Acknowledgements

We would like to thank Babacar Diop (University of Dakar) for the preparation of the thin sections. We are indebted to Prof. O. Saddiqi and an anonymous reviewer for their fruitful remarks which helped improve the manuscript, and to Dr. Mapeo (EiC) for his help in the English polishing. This is an IGCP638-Unesco contribution.

References

Abouchami, W., Boher, M., Michard, A., Albarède, F.N.T., 1990. A Major 2.1 Ga event of mafic magmatism in West Africa : an early stage of crustal accretion. *Journal of Geophysical Research,* 95, 17605-17629.

Aïfa, T., Dabo, M., 2011. Airborne survey to investigate mineralizations within eastern Senegal. *23rd Colloquium of African Geology,* Jan. 8-14, Johannesburg, South Africa, p.3 (Abstr. vol. Suppl.).

Ama Salah, I., Liégeois, J.P., Pouclet, A., 1996. Evolution d'un arc insulaire océanique birimien précoce au Liptako nigérien (Sirba): géologie, géochronologie et géochimie. *Journal of African Earth Sciences,* 22, 235-254.

Attoh, K., Evans, M.J., Bickford, M.E., 2006. Geochemistry of ultramafic - rodingite rock association in the Paleoproterozoic Dixcove greenstone belt, southwestern Ghana. *Journal of African Earth Sciences,* 45, 333-346.

Bassot, J.P., 1966. Etude géologique du Sénégal oriental et de ses confins guinéo-maliens. *Mémoires BRGM*, 40, 1-332.

Bassot, J.P., 1987. Le complexe volcano-plutonique calco-alcalin de la rivière Daléma (Est Sénégal) : discussion de sa signification géodynamique dans le cadre de l'orogénie éburnéenne (Protérozoïque inférieur). *Journal of African Earth Sciences,* 6(1), 109-115.

Bassot, J.P., 1997. Albitisations dans le Paléoprotérozoïque de l'Est Sénégal : relations avec les minéralisations ferrifères de la rive gauche de la Falémé. *Journal of African Earth Sciences,* 25(3), 353-367.

Bassot, J.P., Caen-Vachette, M., 1984. Données géochronologiques et géochimiques nouvelles sur les granitoïdes de l'Est du Sénégal. Implication sur l'histoire géologique du Birimien dans cette région. *In*: Klerkx, J., Michot, J. (Eds.), *Géologie Africaine*. Tervuren, Belgique, 191-209.

Bassot, J.P., Dommanget, A., 1986. Mise en évidence d'un accident majeur affectant le Paléoprotérozoïque inférieur des confins sénégalo-maliens. *Compte Rendu Académie des Sciences,* Paris, 302, 1101-1106.

Béziat, D., Bourges, F., Debat, P., Lompo, M., Martin, F., Tollon, F., 2000. A Palaeoproterozoic ultramafic-mafic assemblage and associated volcanic rocks of the Boromo greenstone belt: Burkina Faso: fractionates originating from island-arc volcanic activity in the West African Craton. *Precambrian Research*, 101, 25-47.

576 Blenkinsop, T.G., Schmidt-Mumm, A., Kumi, R., Sangmor, S., 1994. Structural geology of
577 the Ashanti gold mine, Obuasi, Ghana. *Geol. Jahrb.*, D100, 131-153.
578 Block, S., Ganne, J., Baratoux, L., Zeh, A., Parra-Avila, L.A., Jessell, M., Ailleres, L.,
579 Siebenaller, L., 2015. Petrological and geochronological constraints on lower crust
580 exhumation during Paleoproterozoic (Eburnean) orogeny, NW Ghana, West African
581 Craton. *Journal of metamorphic Geology*, 33, 463–494.
582 Boher, M., 1991. Croissance crustale en Afrique de I'Ouest à 2,l Ga. Apport de la géochimie
583 isotopique. *Unpuplished PhD thesis University of Nancy I, France*, 180p.
584 Boher, M., Abouchami, W., Michard, A., Albarède, F., Arndt, N.T., 1992. Crustal growth in
585 West Africa at 2.1 Ga. J. Geophys. Res. 97, 345–369.
586 Bonhomme, M., 1962. Contribution a l'étude géochronologique de la plate-forme de l'Ouest
587 africain. *Géologie Minérale*, 5, *Thesis*, University of Clermont-Ferrand, France, 62p.
588 Cheilletz, A., Barbey, P., Lama, C., Pons, J., Zimmerman, J.L., Dautel, D., 1994. Age de
589 refroidissement de la crouˆ te juvénile birimienne d'Afrique de l'Ouest. Données U–Pb,
590 Rb–Sr et K–Ar sur les formations a` 2.1 Ga du SW-Niger. C.R. Acad. Sci. Paris, 319,
591 435-442.
592 Dabo, M., 2011. Tectonique et minéralisations aurifères dans les formations birimiennes de
593 Frandi-Boboti, boutonnière de Kédougou-Kéniéba, Sénégal. *PhD Thesis,* University of
594 Rennes 1, 233p.
595 Dabo, M., Aïfa, T., 2010. Structural Styles and Tectonic evolution of the Kolia-Boboti
596 sedimentary basin, Kédougou-Kéniéba inlier, eastern Senegal. *Comptes Rendus*
597 *Geoscience,* 342, 796-805.
598 Dabo, M., Aïfa, T., 2011. Late Eburnean deformation in the Kolia-Boboti sedimentary basin,
599 Kédougou-Kéniéba inlier, Sénégal. *Journal of African Earth Sciences*, 60, 106-116.
600 Dabo, M., Aïfa, T., Miyouna, T., Diallo, D.A., 2015. Gold mineralization paragenesis to
601 tectonic structures in the Birimian of the eastern Dialé- Daléma Supergroup, Kédougou-
602 Kéniéba Inlier, Senegal, West African Craton. *International Geology Review*, 58(7), 807-
603 825.
604 Dampare, S.B., Shibata, T., Asiedu, D.K., Osae, S.,Banoeng-Yakubo, B., 2008. Geochemistry
605 of Paleoproterozoic metavolcanic rocks from the southern Ashanti volcanic belt Ghana:
606 petrogenetic and tectonic setting implications. *Precambrian Research*, 162, 403-423.
607 Davis, D.W., Hirdes, W., Schaltegger, U., Nunoo, E.A., 1994. U/Pb age constraints on
608 deposition and provenance of Birimian and goldbearing Tarkwaian sediments in Ghana,
609 West Africa. *Precambrian Research,* 67, 89-107.

Debat, P., Nikiéma, S., Mercier, A., Lompo, M., Béziat, D., Bourges, F., Roddaz, M., Salvi, S., Tollon, F., Wenmenga, U., 2003. A new metamorphic constraint for the Eburnean orogeny from Paleoproterozoic formations of the Man shield (Aribinda and Tampelga countries, Burkina Faso). *Precambrian Research*, 123, 47-65.

Delor, C., Couëffé, R., Goujou, J.C., Diallo, D.P., Théveniaut, H., Fullgraf, T., Ndiaye, P.M., Dioh, E., Blein O., Barry, T.M.M., Cocherie, A., Le Métour, J., Martelet, G., Sergeev, S., Wemmer, K., 2010. Notice explicative de la carte géologique à 1/200 000 du Sénégal, feuille Saraya-Kédougou Est. Ministère des Mines, de l'Industrie, de l'Agro-Industrie et des PME, Direction des Mines et de la Géologie, Dakar.

Dia, A., 1988. Caractère et signification des complexes magmatiques et métamorphiques du secteur de Sandikounda-Laminia (Nord de la boutonnière de Kédougou, Est du Sénégal): un modèle géodynamique du Birimien de l'Afrique de l'Ouest. *Thèse Université Dakar*, Sénégal, 350p.

Dia, A., van Schmus, W.R., Kröner, A., 1997. Isotopic constraints on the age and formation of a Palaeoproterozoic volcanic arc complex in the Kedougou inlier, eastern Senegal, West Africa. *J. Journal of African Earth Sciences,* 24(3), 197-213.

Diallo, D.P., 1994. Caractérisation, d'une portion de croûte d'age protérozoïque inférieur du craton Ouest africain: Cas de l'encaissant des granitoïdes dans le Supergroupe de Mako (boutonnière de Kédougou) - implications géodynamiques. *Thèse Université Cheikh Anta Diop Dakar*, Sénégal, 466p.

Diallo, D.P., Debat, P., Rocci, G., Dia, A., Ngom, P.M., Sylla, M., 1993. Pétrographie et géochimie des roches méta-volcano-detritiques et méta-sédimentaires du Protérozoïque inférieur du Sénégal oriental dans le Supergroupe de Mako (Sénégal, Afrique de I'Ouest): incidences géotectoniques. *Publications Occasionnelles CIFEG*, 23, 1115.

Diallo, D.P., 2001. Lithostratigraphie du Supergroupe de Mako (Paléoprotérozoïque du Sénégal oriental). Implications géodynamiques. *Bulletin de l'Institut Fondamental d'Afrique Noire*, Série A, 51(1-2), 33-58.

Dommanget, A., Milési, J.P., Diallo, M., 1993. The Loulo gold and tourmaline-bearing deposit : a polymorph type in the early Proterozoic of Mali (West Africa). *Mineral. Deposita,* 28, 253-263.

Doumbia, S., Pouclet, A., Kouamelan, A., Peucat, J.J., Vidal, M., Delor, C., 1998. Petrogenesis of juvenile-type Birimian (Palaeoproterozoic) granitoids in Central Côte-d'Ivoire, West-Africa: geochemistry and geochronology. *Precambrian Research,* 87, 33-63.

644 Eisenlohr, B.N., Hirdes, W., 1992. The structural development of the early Proterozoic
645 Birimian and Tarkwaian rocks of southwest Ghana, West Africa. *Journal of African Earth*
646 *Sciences,* 14, 313-325.
647 Feybesse, J.L., Milési, J.P., Johan, V., Dommanget, A., Calvez, J.Y., Boher, M., Abouchami,
648 W., 1989. La limite Archéen-Protérozoïque inférieur de l'Afrique de l'Ouest : une zone de
649 chevauchement majeur antérieure à l'accident de Sanssandra : l'exemple des régions
650 d'Odienné et de Touba (Côte d'Ivoire). *Compte Rendu Académie des Sciences,* Paris, 309,
651 1847-1853.
652 Feybesse, J.L., Billa, M., Guerrot, C., Duguey, E., Lescuyer, J.L., Milesi, J.P., Bouchot, V.,
653 2006. The Palaeoproterozoic Ghanaian province: Geodynamic model and ore controls,
654 including regional stress modeling. *Precambrian Research*, 149, 149-196.
655 Gueye, M., Siegesmund, S., Wemmer, K., Pawlig, S., Drobe, M., Nolte, N., Layer, P., 2007.
656 New evidences for an early Birimian evolution in the West African Craton: An example
657 from the Kédougou-Kénieba Inlier, Southeast Sénégal. *South African Journal of Geology*,
658 110, 511-534.
659 Gueye, M., Ngom P.M., Diène M., Thiam Y., Siegesmund S., Wemmer K., Pawlig S., 2008.
660 Intrusive rocks tectono-metamorphic evolution of the Mako Palaeoproterozoic belt
661 (Eastern Senegal, West Africa). *Journal of African Earth Sciences,* 50, 88-110.
662 Hawkins J.W., 2003. Geology of supra-subduction zones-Implications for the origin of
663 ophiolites. *Geological Society of America Special Papers*, 2003, 373, 227-268.
664 Hirdes, W., Davis, D.W., 2002. U-Pb Geochronology of Palaeoproterozoic rocks in the
665 Southern part of the Kedougou-Kéniéba inlier, Senegal, West Africa: evidence for
666 diachronous accretionary development of the eburnean province. *Precambrian Research*,
667 118, 83-99.
668 Hirdes, W., Davis, D.W., Eisenlohr, B.N., 1992. Reassessment of Proterozoic granitoid ages
669 in Ghana on the basis of U/Pb zircon and monazite dating. *Precambrian Research*, 56, 89-
670 96.
671 Hirdes, W., Davis, D.W., Lüdtke, G., Konan, G., 1996. Two generations of Birimian
672 (Palaeoproterozoic) volcanic belts in north-eastern Côte d'Ivoire (West Africa):
673 consequences for the "Birimian controversy". *Precambrian Research*, 80, 173-191.
674 Jessell, M., Santoul, J., Baratoux, L., Youbi, N., Ernst, R.E., Metelka, V., Miller, J., Perrouty,
675 S., 2015. An updated map of West African mafic dykes. *Journal of African Earth*
676 *Sciences,* 112(B), 440-450.
677 Junner, N.R., 1935. Gold in the Gold coast. *Gold Gost Geol. Surv*., Accra, Mém., 4, 52p.

678 Klemd, R., Hünken, U., Olesch, M., 2002. Metamorphism of the country rocks hosting gold-
679 sulfide-bearing quartz veins in the Palaeoproterozoic southern Kibi-Winneba belt (SE-
680 Ghana). *Journal of African Earth Science*, 35, 199-211.
681 Kretz, R., 1983. Symbols of rock-forming minerals. *American Mineralogist*, 68, 277-279.
682 Ledru, P., Pons, J., Feybesse, J.L., Dommanget, A., Johan, V., Diallo, M., Vinchon, C., 1989.
683 Tectonique transcurrente et évolution polycyclique dans le Birimien, Protérozoïque
684 inférieur du Sénégal-Mali (Afrique de l'Ouest). *Comptes Rendus Académie des Sciences,*
685 Paris, 308, 117-122.
686 Ledru, P., Pons, J., Milési, J.P., Feybesse, J.L., Johan, V., 1991. Transcurrent tectonics and
687 polycyclic evolution in the lower Proterozoic of Senegal-Mali. *Precambrian Research,,*
688 50, 337-354.
689 Leube, A., Hirdes, W., Mauer, R., Kesse, G.O., 1990. The Early Proterozoic Birimian
690 Supergroup of Ghana and some aspects of its associated gold mineralization. *Precambrian*
691 *Research*, 46, 139-165.
692 Liégeois, J.P., Claessens, W., Camara, D., Klerkx, J., 1991.Short-lived Eburnian orogeny in
693 southern Mali. Geology, tectonics, U-Pb and Rb-Sr geochronology. *Precambrian*
694 *Research*, 50, 111-136.
695 Lofgren, G.E., Donaldson, C.H., 1975. Curved branching crystals and differenciation in
696 Comb-Layered Rocks. *Contribution Mineral Petrol.*, 48, 309-319.
697 Loh, G., Hirdes, W., 1999. Explanatory notes for the geological map of Southwest Ghana 1:
698 100 000: Sekondi (0402A) and Axim (0403B) sheets. *Geol. Jb. B.*, 93, 149.
699 Lompo, M., 2009. Geodynamic evolution of the 2.25-2.0 Ga Palaeoproterozoic magmatic
700 rocks in the Man-Leo Shield of the West African Craton. A model of subsidence of an
701 oceanic plateau (Eds.). Paleoproterozoic Supercontinents and Global Evolution.
702 *Geological Society of London, Special Publications*, 323, 231–254.
703 Lompo, M., 2010. Palaeoproterozoic structural evolution of the Man-Leo Shield (West
704 Africa). Key structures for vertical to transcurrent tectonics. *Journal of African Earth*
705 *Sciences,* 58, 19-36.
706 Lüdtke, G., Hirdes, W., Konan, G., Koné, Y., Yao, C., Diarra, S., Zamblé, Z., 1998. Géologie
707 de la région Haute Comoé Nord-feuilles Kong (4b et 4d) et Téhini-Bouna (3a à 3d).
708 *Direction de la Géologie Abidjan Bulletin*, 178p.
709 Lüdtke, G., Hirdes, W., Konan, G., Koné, Y., N'da, D., Traoré, Y., Zamblé, Z., 1999.
710 Géologie de la région Haute Comoé Sud-feuilles Dabakala (2b, d et 4b, d). *Direction de la*
711 *Géologie Abidjan Bulletin*, 176p.

712 Milési, J.P., Diallo, M., Feybesse, J.L., Keita, F., Ledru, P., Vinchon, C., Dommanget, A.,
713 1986. Caractérisation lithostructurale de deux ensembles successifs dans les séries
714 birrimiennes de la boutonnière de Kédougou (Mali-Sénégal) et du Niandan (Guinée);
715 implications giafilogéniques. *Publication CIFEG,* 1986/10, les formations birimiennes de
716 l'Afrique de l'Ouest, 113-121.
717 Milési, J.P., Feybesse, J.L., Ledru, P., Dommanget, A., Quedraogo, M.F., Marcoux, E., Prost,
718 A., Vinchon, C., Sylvain, J.P., Johan, V., Tegyey, M., Calvez, J.Y., Lagny, P., 1989. Les
719 minéralisations aurifères de l'Afrique de l'Ouest. Leurs relations avec l'évolution
720 lithostructurale au Protérozoïque inférieur. *Chronique Recherche Minière,* 497, 3-98.
721 Milési, J.P, Ledru, P., Feybesse, J.L., Dommanget, A., Marcoux, E., 1992. Early Proterozoic
722 ore deposits and tectonics of the Birimian orogenic belt, West Africa. *Precambrian*
723 *Research,* 58, 305-344.
724 Miyashiro, A., 1974. Volcanic rock series in island arcs and active continental margins.
725 *American Journal of Science*, 274, 321-355.
726 Nédélec, A., Bouchez, J.L., 2011. Pétrologie des granites : Structures, cadre géologique.
727 Licence, Master, Capes, Agrégation. *Collection Vuibert*, 306p.
728 Ngom, P.M., 1995. Caractérisation de la croûte birimienne dans les parties centrale et
729 méridionale du Supergroupe de Mako. Implications géochimiques et pétrogénétiques.
730 *Thèse de Doctorat d'Etat,* Université Ch. A. Diop de Dakar, Sénégal, 240p.
731 Ngom, P.M., 1989. Caractères géochimiques des formations Birimiennes du supergroupe de
732 Mako (Sabodala et ses environs). *Journal of African Earth Sciences*, 8, 91-97.
733 Ngom, P.M., Cordani, U.G., Teixeira, W., Janasi, V.D.A., 2010. Sr and Nd isotopic
734 geochemistry of the early ultramafic-mafic rocks of the Mako bimodal volcanic belt of the
735 Kedougou-Kenieba inlier (Senegal). *Arabian Journal of Geosciences*, 3, 49-57.
736 Ngom, P.M., Cissokho, S., Gueye, M., Joron, J.L., 2011. Diversité du volcanisme et évolution
737 géodynamique au Paléoprotérozoïque : exemple du Birimien de la boutonnière de
738 Kédougou-Kéniéba (Sénégal). *Africa Geoscience Review*, 18(1), 1-22.
739 Pawlig, S., Gueye, M., Klischies, R., Schwarz, S., Wemmer, K., Siegesmund, S., 2006.
740 Geochemical and Sr-Nd isotopic data on Birimian formations of the Kédougou-Kénieba
741 Inlier (Eastern Senegal): Implications on the Paleoproterozoic evolution of the West
742 African Craton. *South African Journal of Geology*, 109, 407-423.
743 Pearce, J.A., 1975, Basalt geochemistry used to investigate past tectonic environments on
744 Cyprus. *Tectonophysics*, 25, 41 67.

745 Pearce, J.A., 1980, Geochemical evidence for the genesis and eruptive setting of lavas from
746 Tethyan ophiolites. *In* Panayiotou, A. (ed.), Ophiolites: Proceedings, International
747 Ophiolite Symposium, 1979: Nicosia, Cyprus, Geological Survey Department, 261-272.
748 Pearce, J.A., 2003. Supra-subduction zone ophiolites: The search for modern analogues.
749 *Geological Society of America Special Papers*, 373, 269-293.
750 Peters, T., Nicolas, A., Coleman, R.G., 1991. Ophiolite Genesis and Evolution of the Oceanic
751 Lithosphere. Kluwer Academic Publishers, Boston, 903p.
752 Pitcher, W.S., 1993. The nature and origin of granite. *Blackie*, London, 322p.
753 Pons, J., Oudin, C., Valéro, J., 1992. Kinematics of large syn-orogenic intrusions: example of
754 the lower Proterozoic Saraya batholith (eastern Senegal). *Geologische Rundschau,* 81(2),
755 473-486.
756 Pons, J., Barbey, P., Dupuis, D., Léger, J.M., 1995. Mechanism of pluton emplacement and
757 structural evolution of 2.1Ga juvenile continental crust: the Birimian of south-western
758 Niger. *Precambrian Res.*, 70, 281-301.
759 Pouclet, A., Vidal, M., Delor, C., Simeon, Y., Alric, G., 1996. Le volcanisme birimien du
760 nord-est de la Côte d'Ivoire, mise en évidence de deux phases volcano-tectoniques
761 distinctes dans l'évolution géodynamique du Paléoprotérozoïque. *Bulletin de la Société*
762 *géologique de France*, 167(4), 529-541.
763 Pouclet, A., Doumbia, S., Vidal, M., 2006. Geodynamic setting of Birimian volcanism in
764 central Ivory Coast (western Africa) and its place in the Paleoproterozoic evolution of the
765 man Shield. *Bulletin de la Société géologique de France*, 177(2), 105-121.
766 Sylvester, P.J., Attoh, K., 1992. Lithostratigraphy and composition of 2.1 Ga greenstone belts
767 of the West African craton and their bearing on crustal evolution and the Archean-
768 Proterozoic boundary. *Journal of Geology*, 100, 377-393.
769 Taylor, P.N., Moorbath, S., Leube, A., Hirdes, W., 1988. Geochronology and crustal
770 evolution of early Proterozoic granite-greenstone terrains in Ghana/West Africa. *Abstr.*
771 *Int. Conf. Workshop*, Geology of Ghana with Special Emphasis on Gold, Accra, 43-45.
772 Taylor, P.N., Moorbath, S., Leube, A., Hirdes, W., 1992. Early Proterozoic crustal evolution
773 in the Birimian of Ghana: constraints from geochronology and isotope geology.
774 *Precambrian Research*, 56, 97-111.
775 Théveniaut, H., Ndiaye, P.M., Buscail, F., Couëffé, R., Delor, C., Fullgraf, T., Goujou, J.C.,
776 2010. Notice explicative de la carte géologique du Sénégal oriental à 1/500 000. Ministère
777 des Mines, de l'Industrie, de l'Agro-Industrie et des PME, Direction des Mines et de la
778 Géologie, Dakar, 120p.

Vidal, M., Delor, C., Pouclet, A., Siméon, Y., Alric, G., 1996. Evolution géodynamique de l'Afrique de l'Ouest entre 2,2 Ga et 2 Ga: le style "archéen" des ceintures vertes et des ensembles sédimentaires birimiens du nord-est de la Côte d'Ivoire. *Bulletin de la Société géologique de France*, 167(3), 307-319.

Vidal, M., Gumiaux, C., Cagnard, F., Pouclet, A., Ouattara, G., Pichon, M., 2009. Evolution of a Palaeoproterozoic "weak type" orogeny in the West African Craton (Ivory Coast). *Tectonophysics*, 477, 145-159.

Whitney, D.L., Evans, B.W., 2010. Abbreviations for names of rock-forming minerals. *American Mineralogist*, 95, 185-187.

Table captions

Table 1. Previous geochronological data in Mako Supergroup.

Table 2. Mineral assemblages of amphibolites and chloritoschists of Mako.

Figure captions

Figure 1. Kédougou-Kéniéba Inlier (KKI) in the Man shield, southern part of the West African Craton (WAC). **a-** Schematic map of the major Precambrian greenstone belts of the southern part of the WAC (simplified from Pouclet et al., 2006). **b-** Simplified geological map of the Birimian of KKI (modified after Pons et al., 1992). Rectangle delimits the study area. Bo: Boboti; Gm: Gamaye; MTZ: Main Transcurrent Zone; SMF: Senegalo-Malian Fault.

Figure 2. a- Geological map of the Mako Paleoproterozoic greenstone belt. MSZ: Mako Shear Zone; BSZ: Bafoundou Shear Zone. **b,c-** Geological sections (A-A' and B-B') showing the geometrical relations between different lithologies (the vertical scale is approximative). RN7: trunk road n°7.

Figure 3. The ultramafic and mafic rocks of Mako. **a-** Panoramic view of the hills of ultramafic and mafic rocks. **b,c-** Petrography of the ultralmafic rocks visible to the naked eye (**b**) and under polarizing microscope (**c**). **d-** Progressive passage by interpenetration between metagabbro and amygdalae metabasalt massif. **e-** Metagabbro in comb-layered textures showing pyroxene rods ouralitized, arranged in hen foot. **f,g-** Amphibole-gneiss (layered metagabbro) showing through naked eye (**f**) and under microscope (**g**) a foliation with an alternation of light and dark beds. Abbreviations of mineral names according to Witney and Evans (2010). Amp: amphibole, Ep: epidote, Fsp: feldspar, Ol: olivine, Op: opaque mineral, Px: pyroxene, Qz: quartz, Srp: serpentine.

Figure 4. Petrography of mafic rocks of Mako. **a**- Lithological succession between massive metabasalt and in pillow lavas in a quarry north of Mako. **b**- Pillow lavas are presented in variable sizes and shapes. **c**- Basaltic pillow lavas locally contain inclusions of ultramafic rocks. **d**- Metabasalts showing a microlithic texture with plagioclase microlites whereas (**e**) inclusions are grained, made up mainly of serpentine (Srp). **f**- Chloritoschist resulting from the transformation of metabasalts in the shear zone of Bafoundou. Chl: chlorite, Pl: plagioclase.

Figure 5. Ribboned quarzites with an alternation of light and dark beds (**a**), primarily composed of quartz (Qz) with some sericite (Ser) but locally the conglomeratic quarzites show fragments mainly made up of fibrous chlorite (**b**).

Figure 6. Volcanic breccias. **a**- Andesitic breccias showing a cross-bedding (S_0). **b**- Andesitic breccias showing a grain sorting with an alternation of fine levels (Fg) and coarse levels (Cg). **c**- In thin section the fragments show biotite relics. **d**- Andesitic lava with porphyritic microlithic texture with microliths and phenocrysts of plagioclase bathing in a chloritized mesostase. Alkaline quartz and K-feldspars (Afs) fill amygdalaes of the rock. **e**- Rhyolitic breccias showing an alternation of Fg and Cg. **f**- Rhyolite showing a porphyritic microlithic texture with phenocryst of sanidine (Sa) and quartz associated with some biotite (Bt) and sericite (Ser).

Figure 7. Petrography of Eburnean granitoids. **a**- Granodiorite with mafic enclaves of Soukourtou in contact with the orthogneissified microgranite. **b**- Contact between granodiorite and microgranite orthogneissified in thin section. **c**- Mineralogical composition of the Soukourtou granodiorite (Mc: microcline). **c**- Chilled contact in brown crown between the Soukourtou granodiorite and its mafic enclaves. **d,f**- Mineralogical hybrid mixture between granodiorite and mafic enclave, observed under naked eye (**d**) and under microscope (**e**). Enclaves are crossed by quartzo-feldspathic veinlets (Vn).

Figure 8. a- Mottled metagabbro cross-cutting the post-tectonic pink granite of Niéméniké. **b**- The metagabbros are mainly composed of secondary amphiboles (Amp) with some chlorite (Chl) and feldspar (Fsp). **c**- They also cross-cut the quarzite and (**d**) show an undulated foliation (Fo) by crenulation in certain shear zones.

Figure 9. Schematic lithostratigraphic column of the Paleoprotezoic formations of the Mako sector.

It appears a basic ophiolitic complex mainly of tholeiitic nature, topped by mixed volcanic complex with calc-alkali trend. The unit is intruded by three generations of granitoid (early, syn- and post-tectonic). The thickness of the facies is estimated approximatively.

847 **Figure 10.** Distribution of the volcano-plutonic rocks of Mako in Ti-Cr (a) (Pearce, 1975) and
848 Cr-Y (b) (Pearce, 1980) diagrams, respectively (after data of Ngom, 1995).

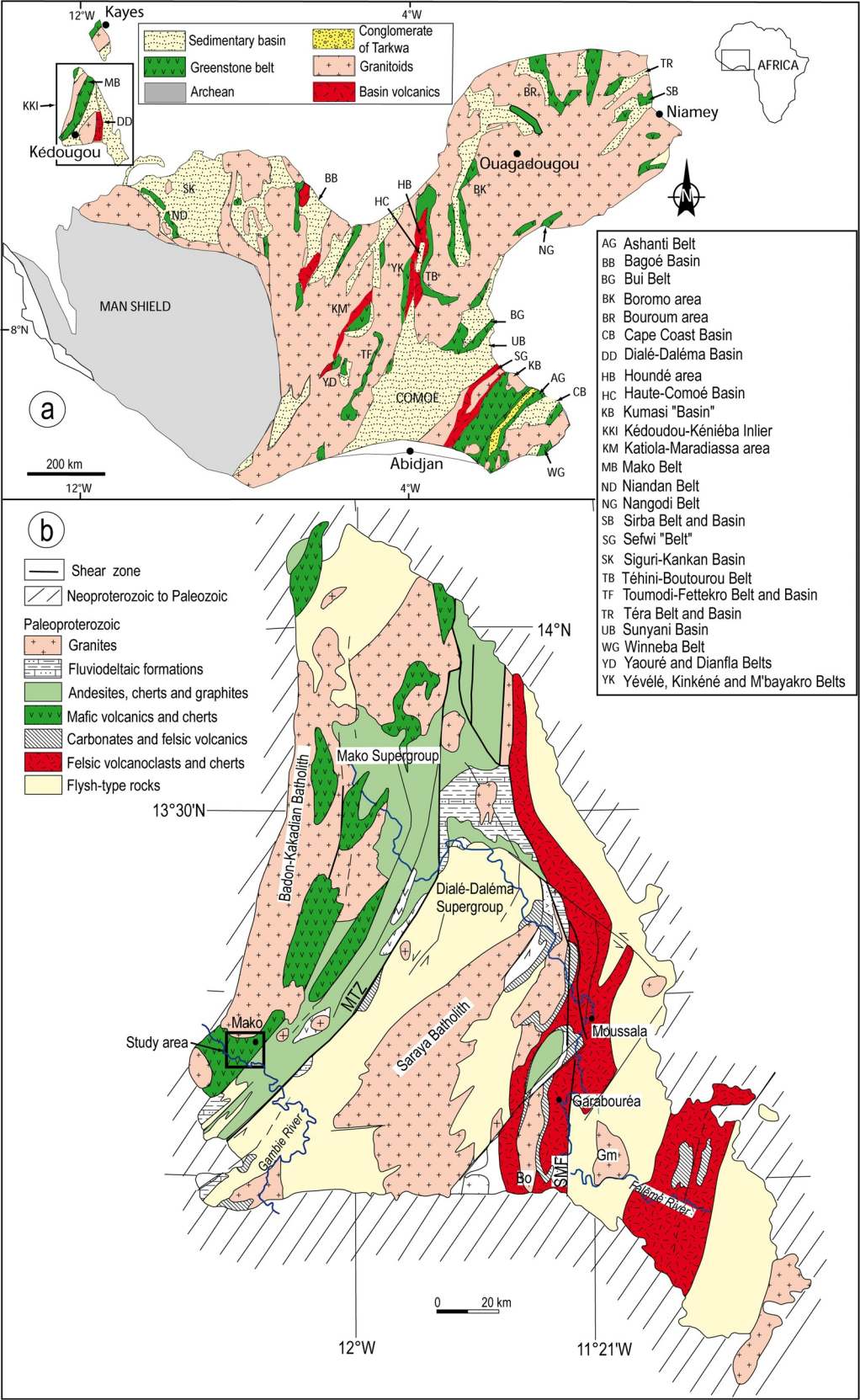
a
b
Kayes
Kédougou
Sedimentary basin
Greenstone belt
Archean
Conglomerate of Tarkwa
Granitoids
Basin volcanics
AFRICA
Niamey
Ouagadougou
Abidjan
MAN SHIELD
COMOE
200 km
12°W
4°W
8°N
AG Ashanti Belt
BB Bagoé Basin
BG Bui Belt
BK Boromo area
BR Bouroum area
CB Cape Coast Basin
DD Dialé-Daléma Basin
HB Houndé area
HC Haute-Comoé Basin
KB Kumasi "Basin"
KKI Kédoudou-Kéniéba Inlier
KM Katiola-Maradiassa area
MB Mako Belt
ND Niandan Belt
NG Nangodi Belt
SB Sirba Belt and Basin
SG Sefwi "Belt"
SK Siguri-Kankan Basin
TB Téhini-Boutourou Belt
TF Toumodi-Fettekro Belt and Basin
TR Téra Belt and Basin
UB Sunyani Basin
WG Winneba Belt
YD Yaouré and Dianfla Belts
YK Yévélé, Kinkéné and M'bayakro Belts
Shear zone
Neoproterozoic to Paleozoic
Paleoproterozoic
Granites
Fluviodeltaic formations
Andesites, cherts and graphites
Mafic volcanics and cherts
Carbonates and felsic volcanics
Felsic volcanoclasts and cherts
Flysh-type rocks
14°N
13°30'N
12°W
11°21'W
Mako Supergroup
Badon-Kakadian Batholith
Dialé-Daléma Supergroup
MTZ
Saraya Batholith
Mako
Study area
Moussala
Garabouréa
Bo
SMFI
Gambie River
Falémé River
0 20 km

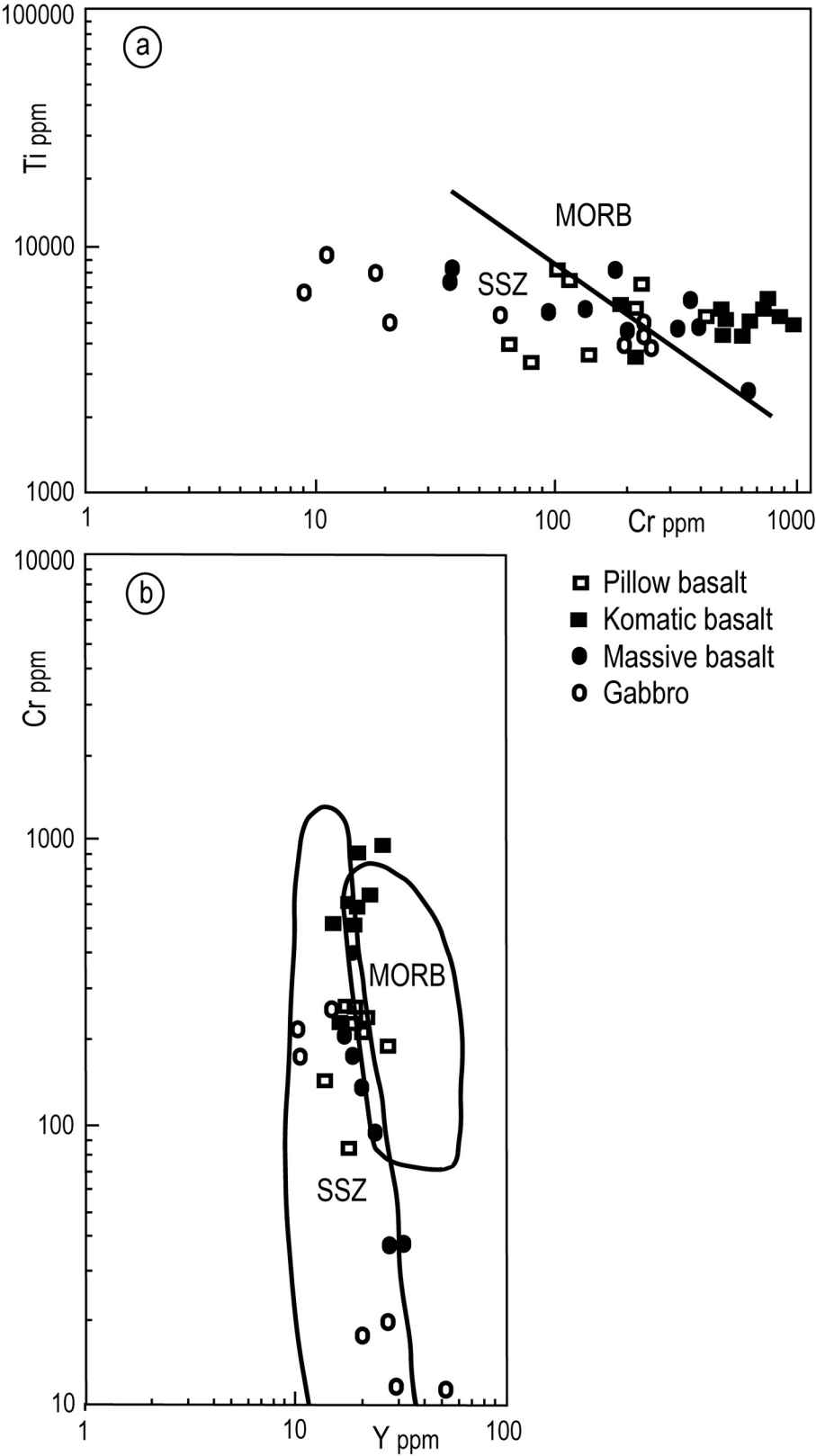
a
Ti ppm
100000
10000
1000
MORB
SSZ
1
10
100
Cr ppm
1000
b
Cr ppm
10000
1000
100
10
MORB
SSZ
1
10
Y ppm
100
Pillow basalt
Komatic basalt
Massive basalt
Gabbro

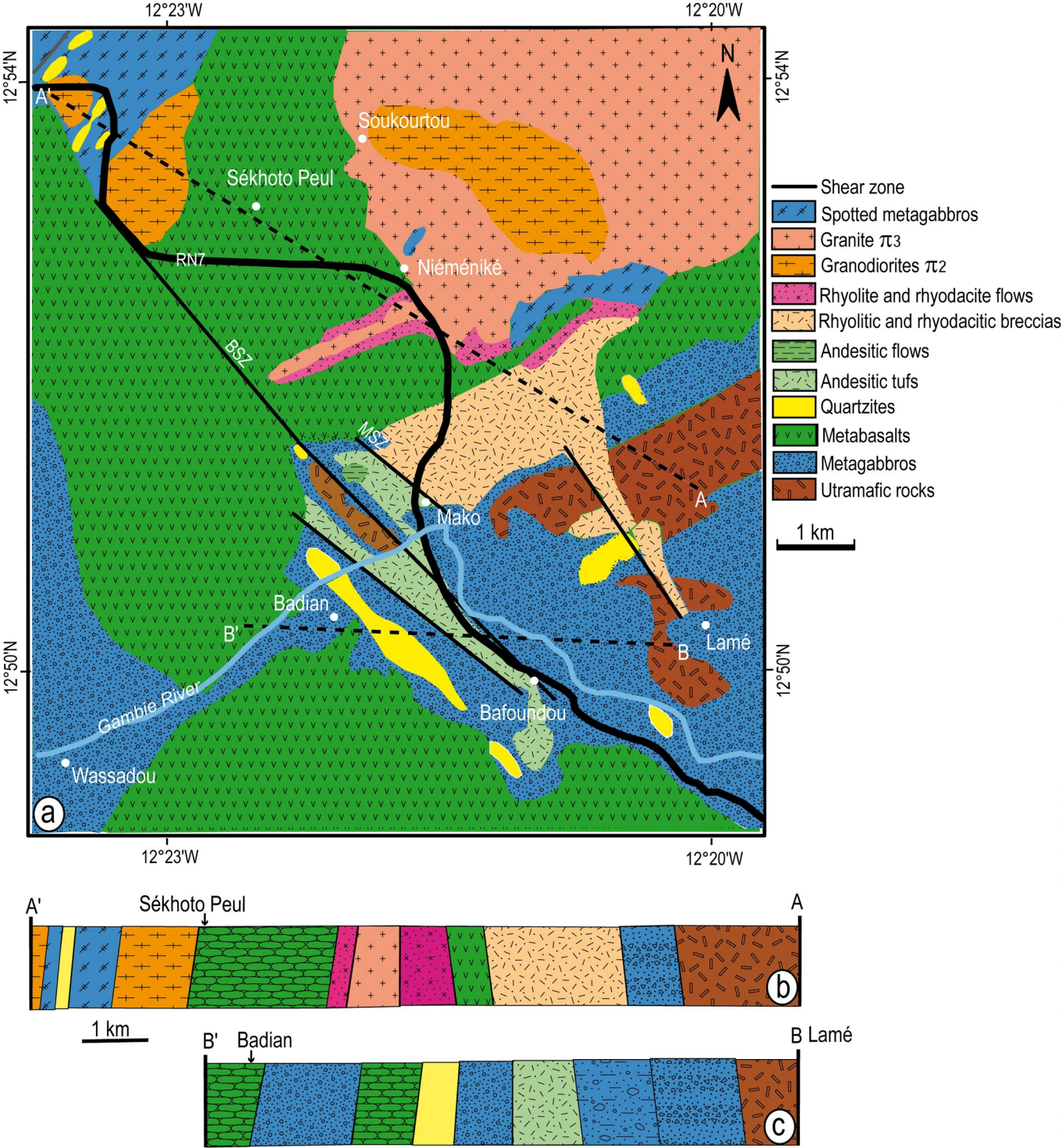
12°23'W
12°20'W
12°54'N
12°50'N
N
A'
A
B'
B
Soukourtou
Sékhoto Peul
Niémènikè
RN7
BSZ
MSZ
Mako
Badian
Lamé
Bafoundou
Gambie River
Wassadou
a
Shear zone
Spotted metagabbros
Granite π3
Granodiorites π2
Rhyolite and rhyodacite flows
Rhyolitic and rhyodacitic breccias
Andesitic flows
Andesitic tufs
Quartzites
Metabasalts
Metagabbros
Utramafic rocks
1 km
A'
Sékhoto Peul
A
b
1 km
B'
Badian
B Lamé
c


a
Bafoundou pillow lavas hills
metagabbros and quartzites complex
Manssaritana peridotites hills
Mako andesitic tufs and lavas
RN7

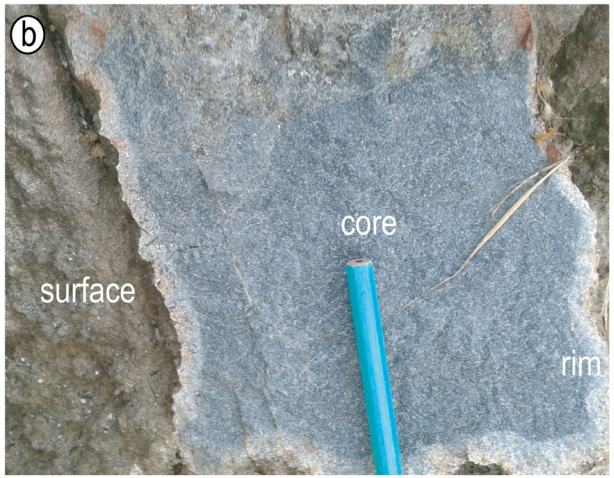
b
core
surface
rim

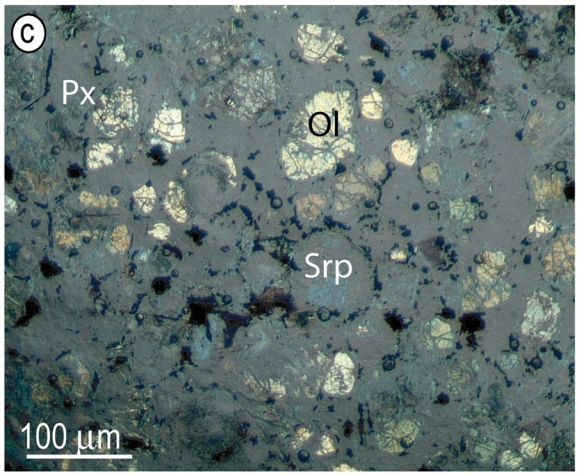
c
Px
Ol
Srp
100 µm


d
metagabbro
amygdalae metabasalt

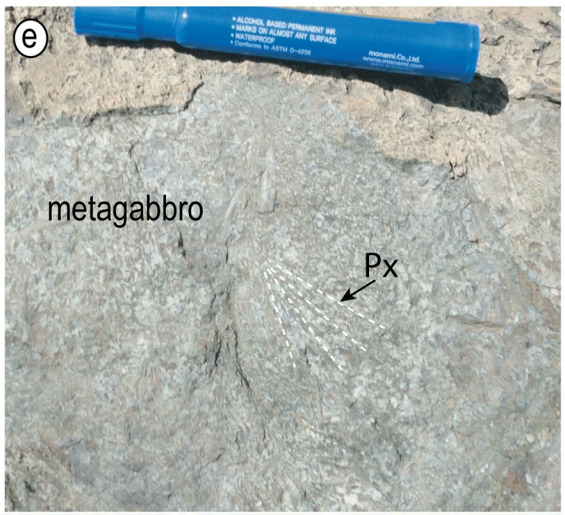
e
metagabbro
Px


f

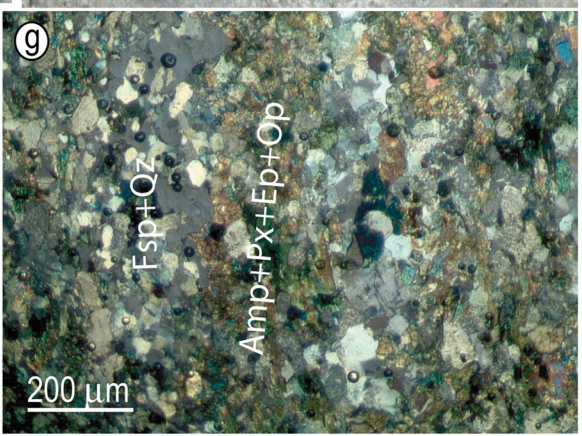
g
Fsp+Qz
Amp+Px+Ep+Op
200 µm

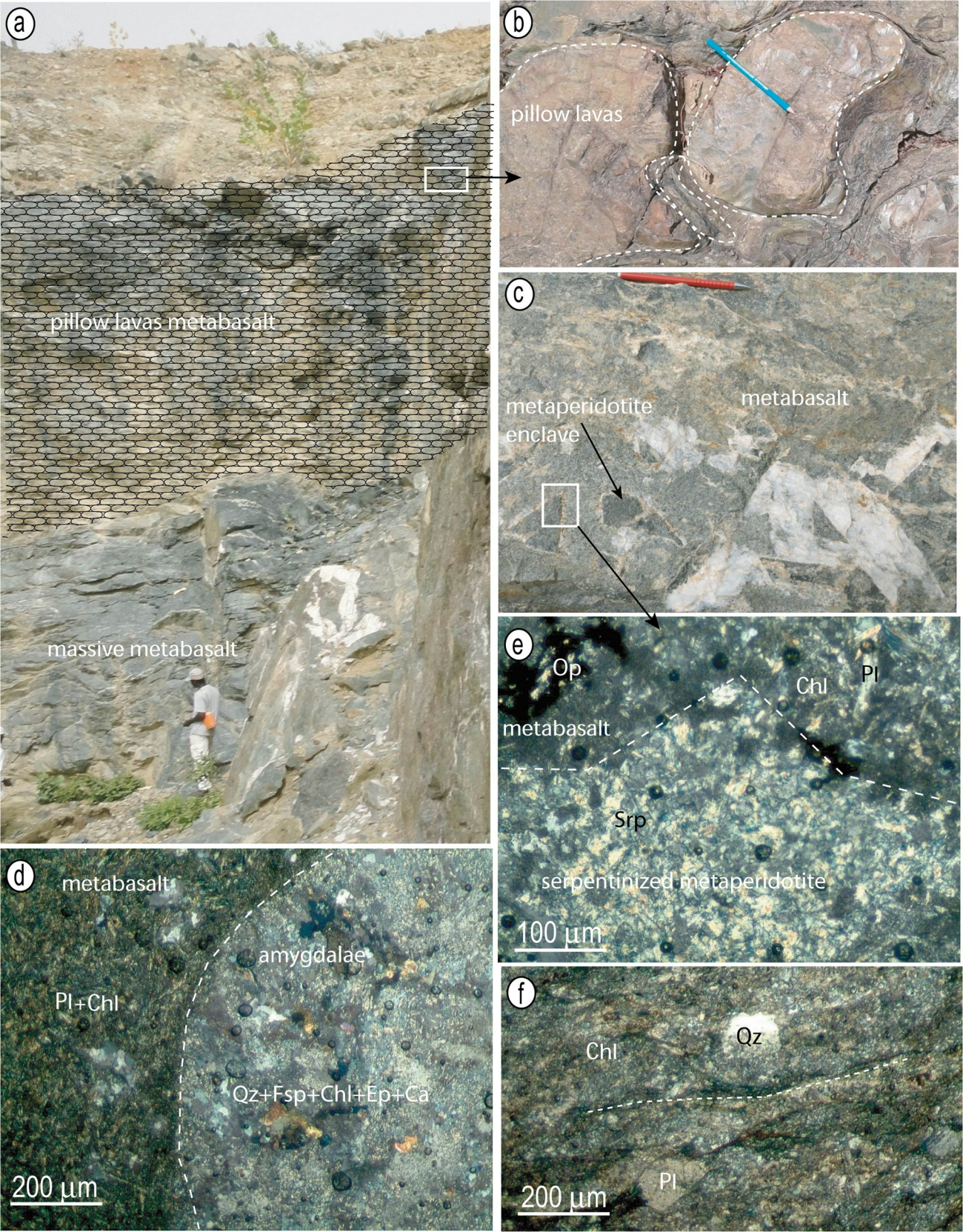
a
pillow lavas metabasalt
massive metabasalt
b
pillow lavas
c
metaperidotite
enclave
metabasalt
e
Op
Chl
Pl
metabasalt
Srp
serpentinized metaperidotite
100 µm
d
metabasalt
amygdalae
Pl+Chl
Qz+Fsp+Chl+Ep+Ca
200 µm
f
Chl
Qz
Pl
200 µm

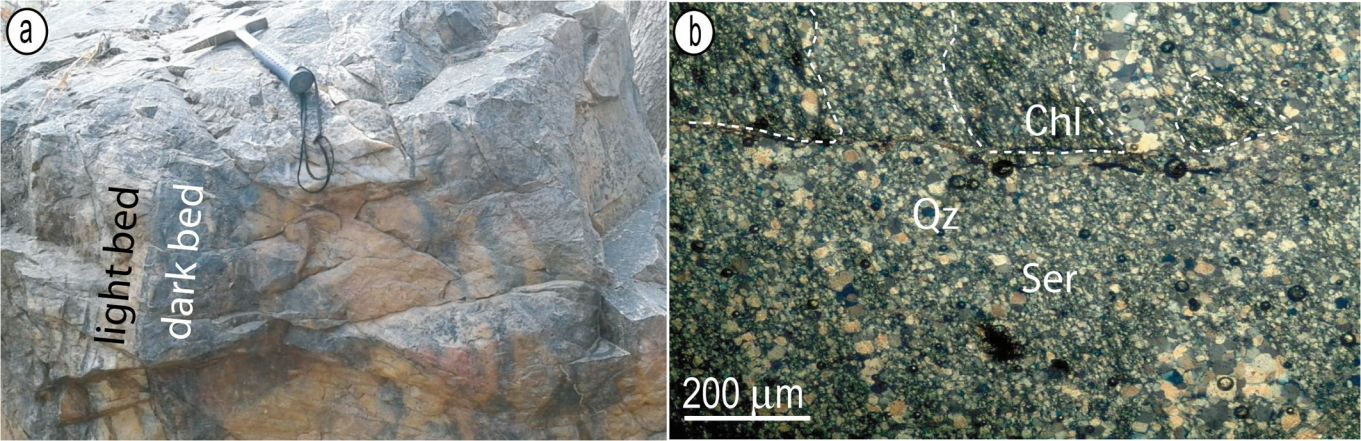
a
light bed
dark bed
b
Chl
Qz
Ser
200 µm

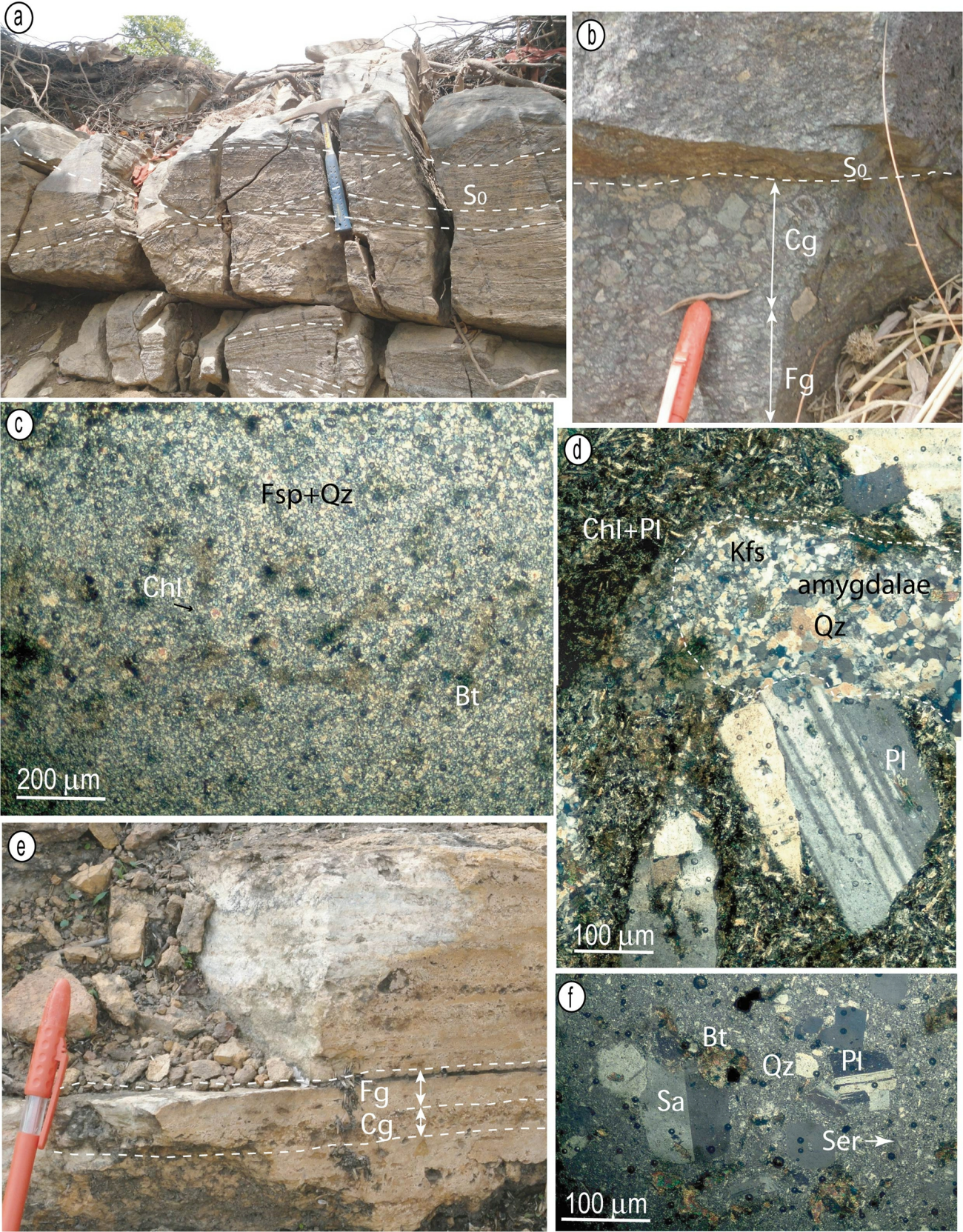
a
S0
b
S0
Cg
Fg
c
Fsp+Qz
Chl
Bt
200 µm
d
Chl+Pl
Kfs
amygdalae
Qz
Pl
100 µm
e
Fg
Cg
f
Bt
Qz
Pl
Sa
Ser
100 µm

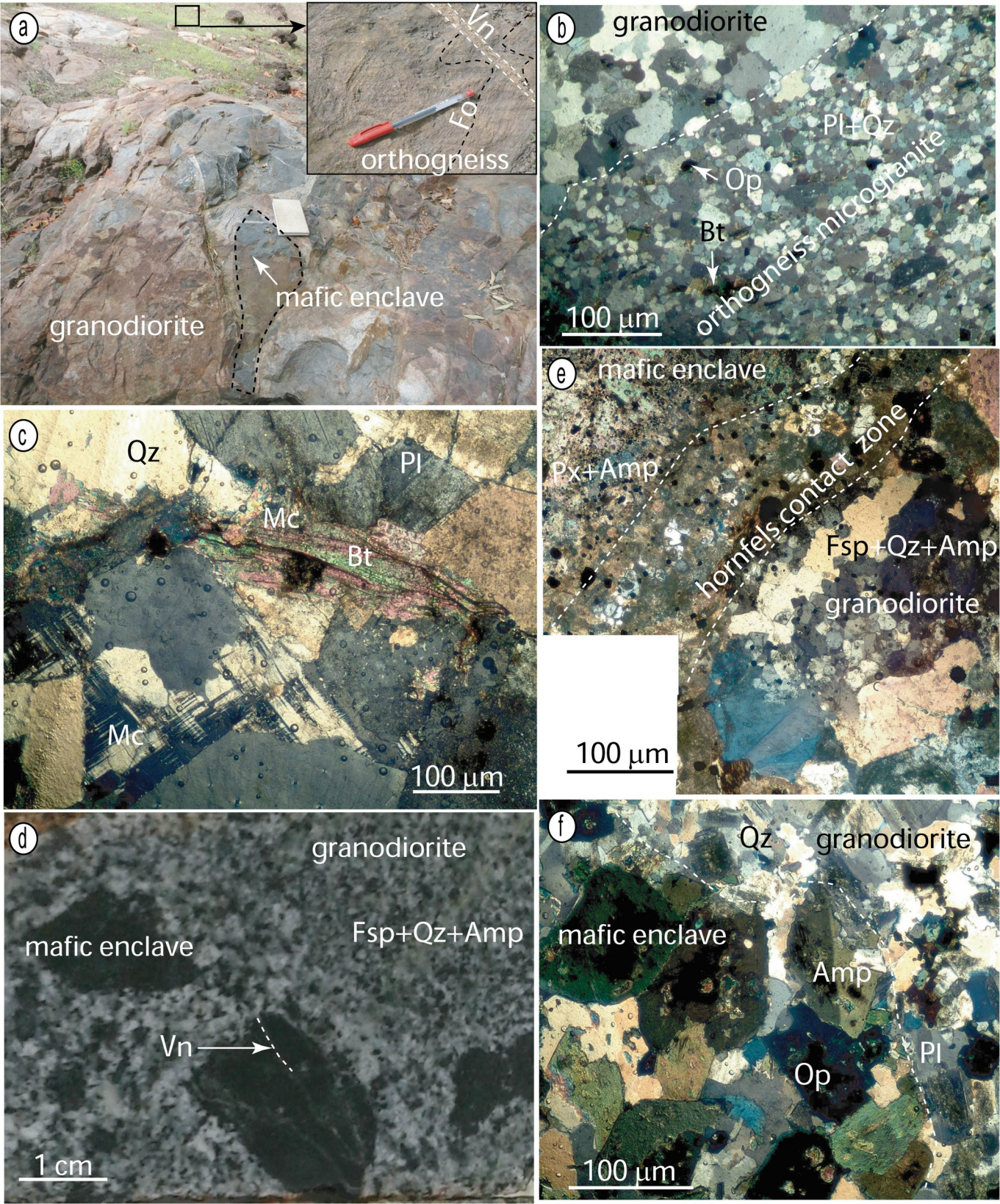
a
Vn
Fo
orthogneiss
mafic enclave
granodiorite
b
granodiorite
Pl+Qz
Op
Bt
orthogneiss-microgranite
100 μm
c
Qz
Pl
Mc
Bt
Mc
100 μm
d
granodiorite
mafic enclave
Fsp+Qz+Amp
Vn
1 cm
e
mafic enclave
Px+Amp
hornfels contact zone
Fsp+Qz+Amp
granodiorite
100 μm
f
Qz
granodiorite
mafic enclave
Amp
Pl
Op
100 μm

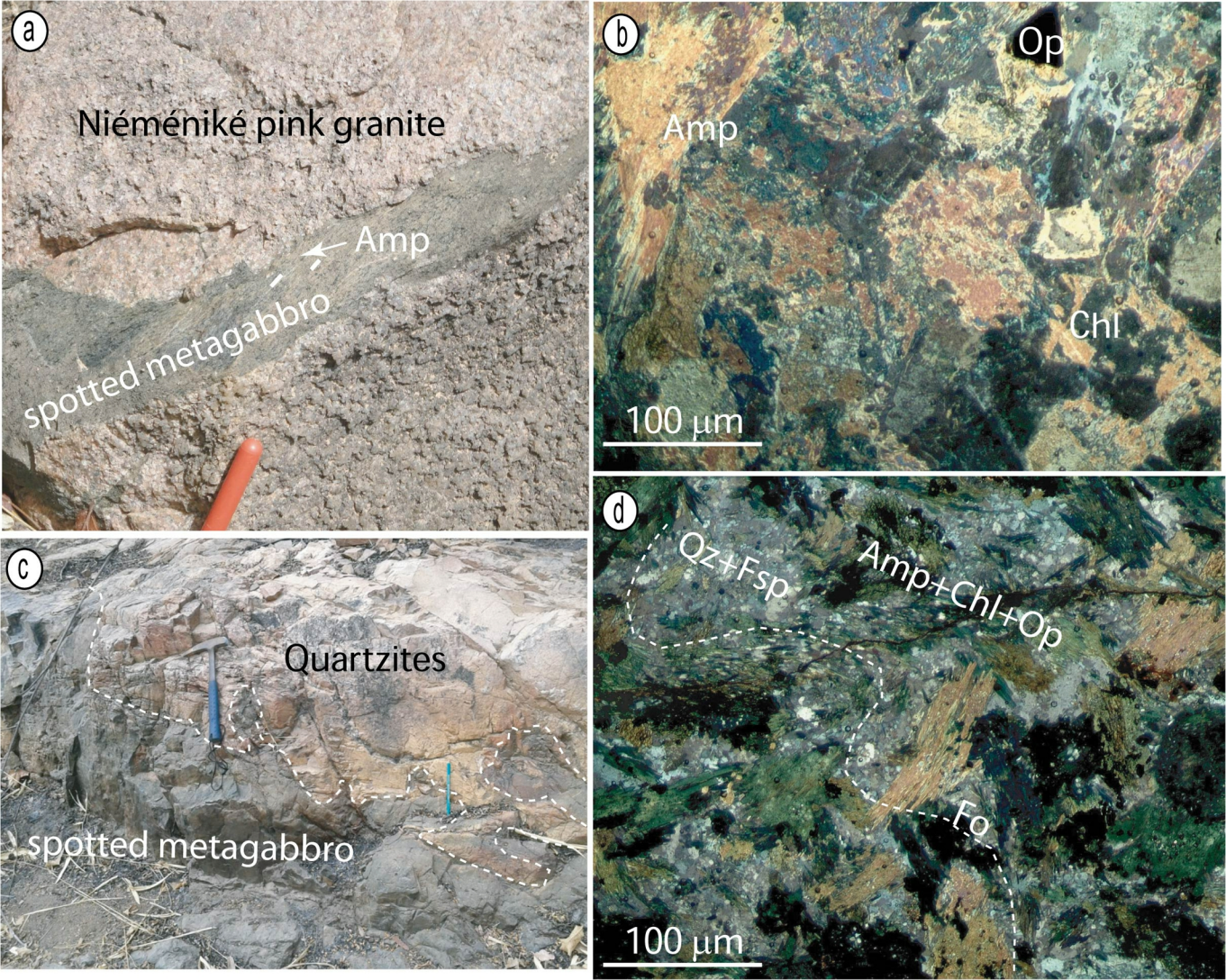
a
Niéméniké pink granite
Amp
spotted metagabbro
b
Op
Amp
Chl
100 µm
c
Quartzites
spotted metagabbro
d
Qz+Fsp
Amp+Chl+Op
Fo
100 µm

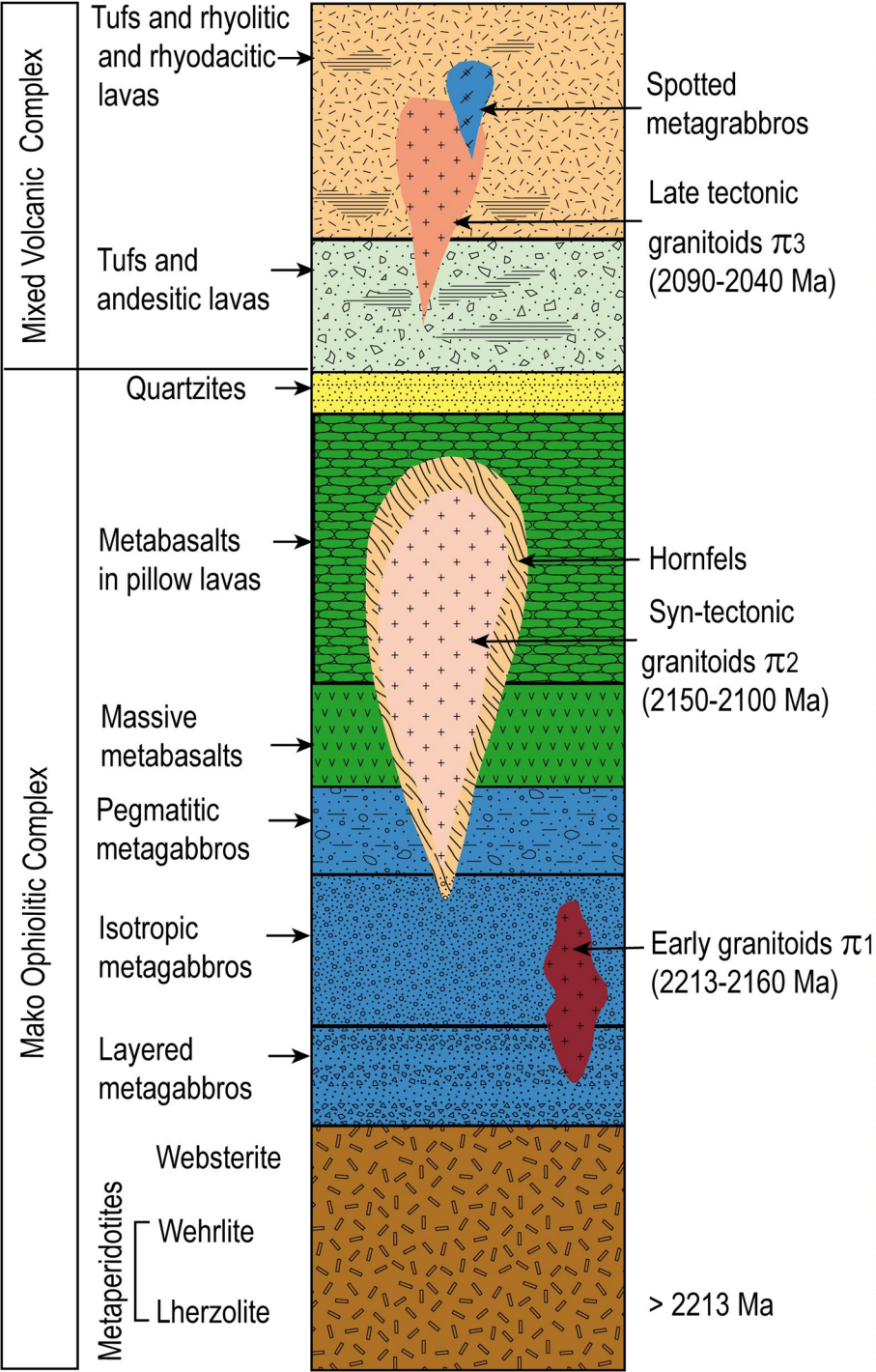
Mixed Volcanic Complex
Mako Ophiolitic Complex
Tufs and rhyolitic and rhyodacitic lavas
Tufs and andesitic lavas
Quartzites
Metabasalts in pillow lavas
Massive metabasalts
Pegmatitic metagabbros
Isotropic metagabbros
Layered metagabbros
Websterite
Metaperidotites
Wehrlite
Lherzolite
Spotted metagrabbros
Late tectonic granitoids π3 (2090-2040 Ma)
Hornfels
Syn-tectonic granitoids π2 (2150-2100 Ma)
Early granitoids π1 (2213-2160 Ma)
> 2213 Ma

Table 1. Previous geochronological data in Mako Supergroup

	Lithology	Petrography	Method	Ages (Ma)	References
Mako Supergroup	Ophiolitic complex	Basalt	Sm/Nd (WR)	2160 ± 16	Boher (1991)
		Basalt	Sm/Nd (WR)	2197 ± 13	Dia (1988)
		Basalt	Pb/Pb (WR)	2195 ± 11	Dia (1988)
		Basalt	Sm/Nd (WR)	2063 ± 41	Abouchami et al. (1990)
	Mixed volcanic complex	Andesites	Sm/Nd (WR)	2160 ± 16	Boher (1991)
Badon-Kakadian batholith intrusions in Mako					
	Granitoid	Granite	Rb/Sr (WR)	2199 ± 68	Bassot and Caen-Vachette (1984)
	Granitoid (Laminia)	Granodiorite	Pb/Pb (Zr)	2105 ± 8	Dia et al. (1997)
	Granitoid (Kaourou)	Granodiorite	Pb/Pb (Zr)	2138 ± 6	Dia et al. (1997)
	Granitoid (Kaourou)	Orthogneiss	Pb/Pb (Zr)	2079 ± 6	Dia et al. (1997)
	Layered plutonic complex (Sandikounda)	Layered gabbro	Pb/Pb (Zr)	2158 ± 8	Dia et al. (1997)
		Tonalite gneiss	Pb/Pb (Zr)	2194± 4	Dia et al. (1997)
		Tonalite gneiss	U/Pb (Zr)	2194± 4	Gueye et al. (2007)
		Diorite gneiss	Pb/Pb (Zr)	2202 ± 6	Dia et al. (1997)
		Amphibolite	Sm/Nd (WR)	2157 ± 67	Dia (1988)
	Granitoid (Mamakono)	Granodiorite	Pb/Pb (Zr)	2076 ± 3	Hirdes and Davies (2002)
	Granitoid (Mamakono)	Granodiorite	U/Pb (Zr)	2067 ± 12	Gueye et al. (2007)
	Granitoid (Badon)	Granodiorite	U/Pb (Zr)	2213 ± 3	Gueye et al. (2007)
	Granitoid (Tinkoto)	Granodiorite	U/Pb (Zr)	2074 ± 9	Gueye et al. (2007)
	Granitoid (Soukouta)	Granodiorite	U/Pb (Zr)	2142 ± 7	Delor et al. (2010)

Zr: zircon, WR: whole rock

Table 2. Mineral assemblages of amphibolites and chloritoschists of Mako

	Amp	Pl	Kfs	Px	Grt	Qtz	Ep	Chl	Bt	Ms	Ca	Ilm
Amphibolites												
AL	+	+	+	+	-	++	++	++	-	++	++	++
AS	+	+	+	+	-	++	++	++	-	++	++	++
OG	+	++	+	-	-	+	++	++	+	++	++	
Chlorito-schists												
CS	++	+	+	-	-	++	++	++	-	++	++	++
TR	-	++	+	-	-	+		-	-	++	++	++
MB	++	++		+	-	++	++	++	-	++	++	
MG	++	++		+	-	++	++	++	-	++	++	
UB	++			+	-	++	++	++	+	++	++	++

(+) primary texture; (++) secondary texture; (-) lacking

Mineral abbreviations following Kretz (1983) and Whitney and Evans (2010); AL : layered amphibolites ; AS : spotted amphibolites ; MB : metabasalts : MG : metagabbros; OG : orthogneiss of Soukourtou ; TR : rhyolitic tuffs of Mako ; CS : chloritoschists; UB : ultrabasites.